INFORMATICS JOURNALS
The Journal of Electrochemical Society of India, *Volume 74, Issue (7&8), October - December 2025; pp. 185–213*
ISSN (Print) : 0013-466X
ISSN (Online) : xxxx-xxxx
DOI: 10.18311/JESCI/2025/55211

Recent Advancements and Challenges in Organic Flow Batteries

Jeet Sharma[1] and Vaibhav Kulshrestha[2*]

[1]Council of Scientific and Industrial Research-Central Salt and Marine Chemicals Research Institute (CSIR-CSMCRI), Gijubhai Badheka Marg, Bhavnagar - 364002, Gujarat, India

[2]Academy of Scientific and Innovative Research (AcSIR), Sector 19, Kamla Nehru Nagar, Ghaziabad - 201002, Uttar Pradesh, India

Abstract

Flow Batteries (FB) are emerging as promising candidates for next-generation electrochemical energy storage systems, offering scalable, safe, and long-duration performance. Conventional FB employing inorganic electrolytes such as vanadium, iron-chromium, zinc, or all-iron chemistries are often constrained by high material costs, electrolyte crossover, and performance decay. In contrast, Organic Flow Batteries (OFB) harness the tunability of redox-active molecules composed of earth-abundant elements (C, H, O, N, halogens, and S), including quinones, nitroxide radicals, heteroaromatic/carbonyl species, and metallocene-based compounds. These molecular systems enable precise control of redox potentials, broad operational voltage windows, and enhanced chemical stability, thereby achieving energy densities and cycling performance comparable to commercial redox flow batteries. This review critically surveys diverse classes of organic redox electrolytes, *viz*., quinones, alloxazines, alloxybenzenes, ferrocenes, viologens, fluorenones, and TEMPO derivatives, along with advances in bipolar and polymeric electrolyte design that underpin next-generation architectures. Strategies for tuning electrochemical windows through host-guest complexation, spacer modification, and charge modulation are discussed to guide molecular engineering. Finally, the review highlights recent progress in solid polymer electrolyte membranes for OFB, emphasising their role in suppressing crossover, improving ion selectivity, and enhancing stability and ionic conductivity, which collectively advance the realisation of durable, high-efficiency organic flow energy systems.

Keywords: Electrochemical Energy Storage, High Energy Density, Organic Redox Electrolytes, Redox Flow Batteries, Stable Redoxmers

1. Introduction

Among various energy storage technologies, Redox Flow Batteries (RFB) have emerged as the most viable and sustainable solution for electrochemical energy storage at the Mega Watt-hour (MWh) to Tera Watt-hour (TWh) scale[1]. Unlike solid-state batteries, RFB store energy in externally housed liquid electrolytes and operate through the independent scaling of power output and energy capacity, hence they are described as power-energy decoupled systems[2]. The long operational life of RFB is primarily governed by the performance and stability of Redox-Active Molecules (RAM) and Polymer Electrolyte Membranes (PEM), rather than by the electrode chemistry itself. This structural independence renders RFB a technologically ready and flexible option to mitigate the intermittency challenges of renewable energy sources, particularly when installation costs are minimised. In contrast, commercial lithium-ion batteries rely on lithium intercalation in transition-metal-based layered oxides or phosphates as cathode materials. These chemistries are expected to face critical raw-material constraints within the coming decade, especially under projected TWh-scale energy demands[3].

**Email: vaibhavk@csmcri.res.in*

Since Thaller first proposed the iron-chromium RFB concept in 1974, the field has undergone substantial advancements in electrolyte chemistry, system design, and electrochemical cell engineering. Inspired by this principle, Smith *et al.* introduced OFB based on redox-active quinones, marking a transformative step toward sustainable, metal-free electrochemical storage[4]. OFB offer key advantages, including minimal electrolyte crossover, high ion selectivity, and excellent cycling stability with consistent efficiencies. Consequently, research and development efforts are increasingly directed toward OFB as environmentally benign and scalable alternatives to conventional inorganic systems. Notably, robust polymer membranes with intrinsic acid-alkaline stability can often be adopted directly in OFB without requiring complex ion-gradient architectures.

The significance of this review lies in its comprehensive analysis of the latest developments and emerging opportunities in OFB technology for sustainable grid-scale energy storage. The review is structured around the following key themes:

1. Advancements in organic RAM design for high energy density and capacity retention through strategic molecular modifications and stability enhancement under extreme pH conditions.
2. Exploration of commercial PEM and prospects for alternative ion-conducting materials, particularly hydrocarbon-based PEM, polymers of intrinsic microporosity, and 2D-reinforced structures featuring superior electrochemical performance and extended chemical durability.
3. Mechanistic understanding and modification of electrodes, focusing on their interfacial behaviour and performance enhancement in OFB environments.
4. Benchmarking of materials (RAM and PEM) and evaluation of key performance metrics for representative OFB systems.
5. Future directions and commercialisation outlook for OFB as demand-specific, sustainable electrochemical energy storage technologies.

2. Organic Flow Batteries (OFB)

The performance, operational behaviour, and classification of RFB are primarily dictated by the nature of the RAM employed for energy storage. RFB utilising redox-active transition-metal salts such as Vanadium (V), Chromium (Cr), Iron (Fe), Copper (Cu), Zinc (Zn), and Tin (Sn), as well as polyoxometalates, heteropolyacids, and polysulfide-polyhalide couples, are collectively termed as Inorganic Flow Batteries (IFB). In contrast, the FB employing redox-active organic molecules like quinones, viologens, nitroxide radicals, heteroaromatic or carbonyl compounds, metallocene-based sandwich complexes and their functional derivatives are categorised as OFB[5]. Recently, Hybrid Flow Batteries (HyFBs), which integrate both inorganic and organic RAM, have emerged as promising alternatives that combine the high stability of inorganic systems with the structural tunability and sustainability of organic molecules.

Figure 1 illustrates the general working principle and cell configuration of an OFB, including its essential components such as pumps, pipelines, and stack assembly, which collectively define its power and energy characteristics. Akin to conventional RFB, OFB stores and delivers energy through redox reactions of solubilised active species in separate anolyte and catholyte reservoirs; however, their distinct feature lies in the complete replacement of inorganic salts with organic redoxmers. The high molecular design flexibility and excellent chemical processability of organic compounds impart OFB with remarkable operational stability, high coulombic efficiency, and the potential for low-cost, metal-free energy storage, positioning them as credible successors to second-generation vanadium RFB.

Despite these advantages, one of the most persistent challenges in OFB research arises from the low solvation energy and hydrophobicity of many organic cores, which restrict molecular solubility and consequently limit energy density, specific capacity, and electrolyte utilisation[6]. Addressing these issues has driven extensive research efforts into the design of advanced redox molecules and compatible ion-exchange membranes to realise scalable, high-performance organic flow systems.

2.1 Classification of OFB

Based on the electrochemical identity of the RAMs in the two electrolyte compartments, OFB are broadly divided into symmetric and asymmetric configurations. Symmetric OFB (SOFBs) employ identical electroactive species in both tanks, ensuring intrinsic chemical compatibility and eliminating crossover-induced degradation. Whereas Asymmetric OFB (AOFBs) utilise different redox pairs in the catholyte and anolyte (where Red ≠ Red' and Ox ≠ Ox' , as illustrated in Figure 1),

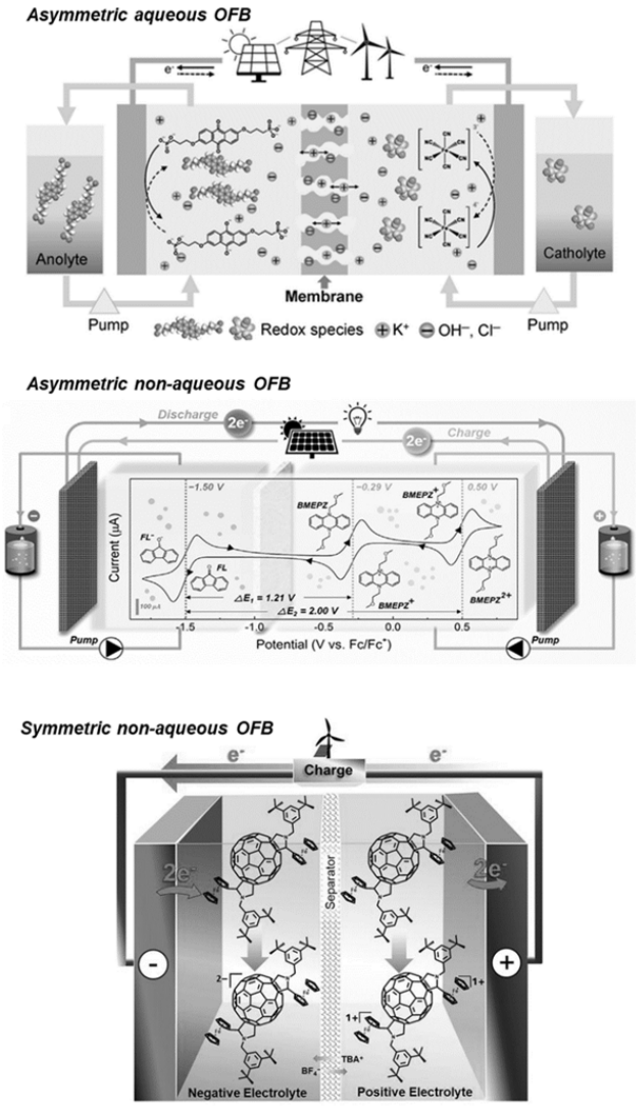


Figure 1. Schematic illustration of the operational principle of Organic redox Flow Batteries (OFB) in a single-cell configuration, depicting both symmetric and asymmetric systems. The membrane-electrolyte assembly consists of serially arranged layers of "Anolyte | Membrane | Catholyte" compartments, typically stacked in multiples (>1) to achieve the desired power output and energy capacity[8-10].

enabling wider voltage windows but at the expense of increased chemical complexity. In certain architectures, volumetric asymmetry ($V_{catholyte} \neq V_{anolyte}$) is also employed to balance charge capacity or mitigate solubility limits. While such strategies have proven beneficial in inorganic systems, they may induce electrolyte crossover and volume imbalance in OFB, leading to faster capacity fading and reduced operational life. Consequently, SOFB are generally regarded as the more durable and self-balancing alternative[7]. Furthermore, OFB are classified according to the nature of the supporting electrolyte into two major categories, namely, (i) Aqueous OFB, which operate in acidic, alkaline, or pH-neutral environments, and (ii) Non-aqueous OFB, which employ organic solvents such as acetonitrile, dimethoxymethane, hexane, or 1-propanol.

A comparative summary of representative RFB technologies, their energy storage chemistries, and characteristic examples is presented in Table 1. Collectively, these classifications outline the foundational framework of flow battery technologies and highlight the growing prominence of OFB as sustainable, structurally tunable, and environmentally benign energy storage systems poised to meet future grid-scale demands. A comprehensive discussion on different OFB is presented in Section 3.

2.2 Pivotal Components of OFB

The electrochemical configuration of various OFB systems is illustrated in Figure 2. A typical OFB assembly comprises three primary components that collectively determine its efficiency, performance, durability, and practical applicability, *viz.* (i) RAM, (ii) A polymer electrolyte separator (ion-exchange or polyelectrolyte membrane, PEM), and (iii) Carbon- or graphite-based electrodes, which serve as the active sites for redox reactions[21]. In addition to these core elements, the complete flow-cell system also includes auxiliary components such as electrolyte reservoirs, circulation pumps, flow distributors, photovoltaic interfaces, and control or regulation modules, all of which contribute to maintaining operational stability and energy management.

2.2.1 Redox-active Molecules for OFB

RAM are organic compounds capable of undergoing highly reversible redox transformations between two or more stable oxidation states over a defined potential window, as typically confirmed by cyclic voltammetry. These distinct charge and discharge states can be regarded as molecular "on" and "off" configurations, reversibly interconverted under an applied potential with rapid electron-transfer kinetics. In OFB, RAM functions as the core charge-storage media and serves as the primary determinant of electrochemical performance, capacity, and long-term stability.

Table 1. Classification of RFB and OFB[7]

<table>
<tr><td colspan="4">Broad Categories of Redox Flow Battery (FB) Technology[A] (All liquid-based batteries)</td></tr>
<tr><td colspan="2">Inorganic FB (IFB): Uses inorganic salts or complexes of transition metal ions as redox energy storage medium.</td><td colspan="2">Organic FB (OFB): Uses organic species (viz quinones, TEMPO, bipolar RAM, metallocenes, viologens, fluorenones, etc. or complexes as redox energy storage medium.</td></tr>
<tr><td colspan="4">Based on the catholyte and anolyte constituents[B]</td></tr>
<tr><td>Symmetric IFB: Identical redox active sites in electroactive species. [C]</td><td>Asymmetric IFB: Unidentical redox active sites in electroactive species.</td><td>Symmetric OFB: Identical redox active sites in organic electroactive species.</td><td>Asymmetric OFB: Unidentical redox active sites in organic electroactive species. [D]</td></tr>
<tr><td rowspan="2">e.g., All-Vanadium IFBs (VRFB), All Iron IFB (IIFB), soluble lead acid batteries, etc.</td><td rowspan="2">e.g., Cerium-Zinc FB, Iron-Chromium FB, Zinc-Bromine FB, etc.</td><td>e.g., RIBOTEMPO[E‡]</td><td>e.g., N-Methyl phthalimide anolyte and 2,5-di-tert-butyl-1-methoxy-4-[2′-methoxyethoxy] benzene catholyte [F], methyl viologen (anolyte) and 4-hydroxy-2,2,6,6-tetramethylpiperidin-1-oxyl (catholyte)[G], 4-[3-(trimethylammonio)propoxy]-2,2,6,6-tetramethylpiperidine-1-oxyl chloride as catholyte[G], etc.</td></tr>
<tr><td colspan="2">Based on the nature of supporting electrolyte employed
(In OFB, the supporting electrolyte can be of organic solvents like Acetonitrile, Dimethyl sulfoxides, Ethers, etc., then such OFB are called non-aqueous OFB. While the OFB which uses acid, base and salt-based electrolytes such as dil. H_2SO_4, brine, dil. NaOH, dil. KOH, etc. are called Aqueous OFB.)</td></tr>
<tr><td colspan="4">Footnotes: [A] FB having one flow component and another redox solid component are also called hybrid RFB, [B] Asymmetric volume ratios are used to improve the capacity retention of FB system, [C] mostly acidic pH electrolytes are used and alkaline IFB are also reported with Zinc-Manganese redoxmers, all Iron-FBs and Sulphur-Iron RFB, [D] can be all organic RAMs or inorganic-organic RAMs in identical supporting electrolytes, [E] in aqueous medium and mostly in organic electrolytes (i.e., non-aqueous FB systems),[F] non-aqueous AOFB,[G] aqueous AOFB.
Abbreviation: TEMPO: (2,2,6,6-tetramethylpiperidin-1-yl)oxidanyl, RIBOTEMPO: Riboflavin-TEMPO.</td></tr>
</table>

During redox cycling, electron transfer occurs *via* a tunnelling or hopping mechanism, forming the fundamental basis for energy storage through controlled electron loss and gain. The overall performance of a RAM is governed by a delicate balance between molecular solubility, electrochemical stability, resistance to oxidative degradation or parasitic reactions, and viscosity in the supporting electrolyte. High molar solubility and low viscosity are particularly desirable, as excessive solution viscosity hampers mass transport and electron transfer kinetics, thereby increasing the energy demand for electrolyte circulation.

Although many organic molecules inherently exhibit redox activity, recent research emphasises the rational molecular design of RAMs to enhance solubility, voltage stability, and achievable energy density. The polarity of functional groups significantly influences solubility in electrolytes, generally following the order: Amide ($-CONH_2$) > acid (-COOH) > alcohol (-OH) > aldehyde (-CHO) ≈ ketone (C=O) > amine ($-NH_2$) > ester (-COOR) > ether (-OR) > alkane (-R). Consequently, polar solvents preferentially dissolve polar redox molecules, consistent with the "like-dissolves-like" principle.

Based on their charge-storage mechanism, RAM are categorised as n-type, p-type, or bipolar species, the latter bearing both donor and acceptor motifs within a single molecule. Charge compensation during redox cycling is maintained by counterions in the electrolyte. The active redox centres are typically element-specific and dictate the electron-transfer pathway. For example, nitrogen-based motifs such as azo, imine, and nitrile groups are commonly n-type, while tertiary amines act as p-type scaffolds. Similarly, sulphur-containing groups (thiols, disulfides, sulfoxides), oxygen-based functionalities (ethers, ketones), and metallocene complexes (*e.g.*, cyclopentadienyl sandwich compounds) exhibit distinct redox behaviours.

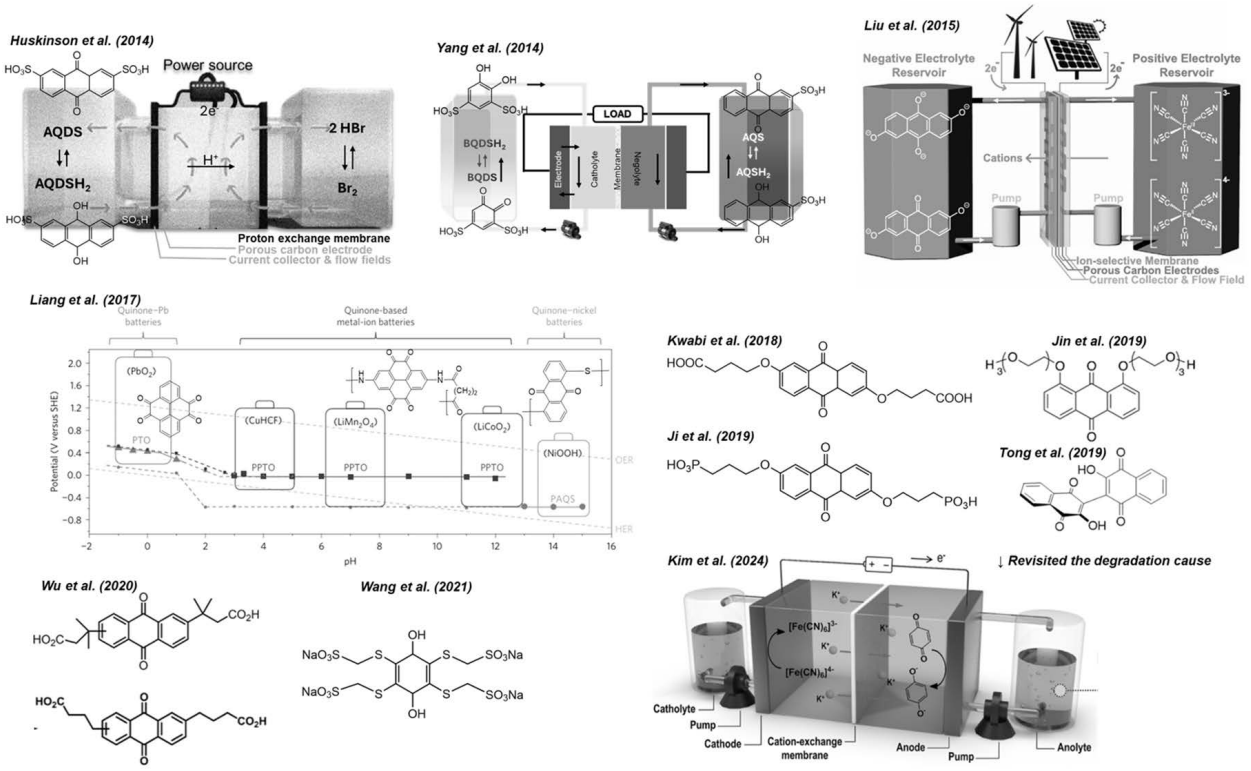


Figure 2. Recent advanced organic flow cells based on the quinones and their derivatives for high performance electrochemical energy storage (trends in strategic functionalisation to acquire high-performance RAM)[11-20].

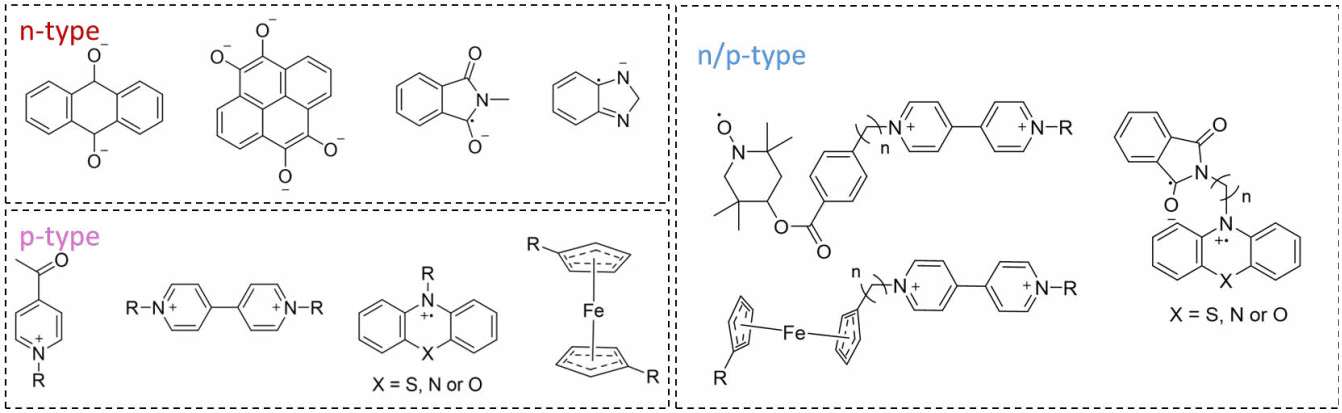


Figure 3. Examples of some n-type, p-type and n/p- (or bipolar) type RAM for OFB.

To date, approximately 56 key redox-active molecular scaffolds have been reported, with most new derivatives being structural modifications of these archetypes. Emerging research has also introduced Deep Eutectic Solvents (DES), ionic liquid-based molecules, and redox-active polypeptides as next-generation RAM for OFB applications[22]. These systems leverage asymmetrically charged ions with delocalised electronic structures, resulting in low lattice energies, depressed melting points, and exceptionally high solubilities up to 6M, thereby enabling unprecedented energy densities. Figure 3 summarises the principal structural classes of RAM currently explored for organic flow battery applications.

2.2.2 Separators for OFB

In OFBs, the anolyte and catholyte reservoirs must remain physically isolated to develop an electrochemical

potential across the cell. This separation is achieved using selective membrane materials that effectively prevent the crossover of RAM while permitting only the transport of small counter ions present in the supporting electrolyte. The separator is typically a charged nanoporous film or dense PEM and controls ion migration through ion-selective nanodomains and maintains overall charge balance (*i.e.*, electroneutrality) within the electrochemical system, ensuring stable and efficient operation[23].

PEM have received sustained attention across all electrochemical energy conversion and storage technologies owing to their critical role enabling high energy' conversion efficiency, elevated power density, resistance to fuel leakage (enabled by zero' gap cell architectures), and reliable operation across a wide temperature range, collectively making them indispensable to FB-design. Within RFB, the membrane dictates long' term operational durability by maintaining high ionic conductivity and selectivity while preventing molecular crossover and contamination of electroactive species. To date, only a few flow battery configurations operate without membranes, utilising immiscible redoxlyte[24]. These are called membrane-less RFB. Among various available commercial products, Nafion, a non' reinforced perfluorinated separator developed by Chemours, formerly DuPont™ remain the benchmark standard for both aqueous and non' aqueous RFB[25]. Nafion is composed of a Polytetrafluoroethylene (PTFE) backbone with long perfluorinated side chains terminating in Sulfonic Acid ($-SO_3H$) functional groups. Despite its extensive research maturity and commercial success, the large-scale adoption of Nafion membranes remains economically limited due to their high installation cost (exceeding US$500 m^{-2}), significant electrolyte crossover, and low anion conductivity during OFB operation[26].

Generally, PEM are classified Based on the nature of the immobilised ionic species within the polymer matrix, membranes are broadly categorized as: (i) Cation-Exchange Membranes (CEM), which bear negatively charged groups such as $-SO_3^-$, $-PO_3^{2-}$, or $-CO_2^-$; (ii) Anion-Exchange Membranes (AEM), containing positively charged moieties such as $-NR_3^+$, $-PR_2^+$, or $-SR_2^+$; and (iii) Amphoteric or zwitterionic membranes, which incorporate both ionic functionalities within a single framework[25]. For efficient performance, selective and efficient transport of ions through these permselective membranes is essential. In PEM, the ion migration facilitates through ionic nanochannels serving as nanoconfined pathways preferably via three primary mechanisms *viz* (i) The Grotthuss mechanism (ion hopping, fast), (ii) Segmental or site hopping (moderate), and (iii) The vehicular mechanism (ion diffusion with solvent molecules, slow), corresponding respectively to typical transport modes in CEM and AEM[27]. These migrations are driven either by concentration-gradient diffusion or by electrochemical potential gradients under an applied electric field.

Although dense ion-exchange membranes remain the dominant choice for OFB evaluation, recent advances have shifted attention toward Polymers of Intrinsic Microporosity (PIM) as next-generation membrane materials, offering high selectivity and tunable ion transport[8,28]. It is anticipated that low-cost hydrocarbon-based membranes, combining high conductivity and mechanical durability, could emerge as reliable candidates for large-scale OFB deployment.

2.2.3 Electrode Materials for OFB

In RFB, electrodes act as kinetic mediators for electroactive species, providing electrical connectivity between the non-conducting components of the circuit without directly participating in energy storage. The electrode surface enables the bidirectional tunnelling of electrons (e^-) during the oxidation and reduction of RAM, thereby facilitating charge storage and release[29]. As discussed earlier, RAM, polymer electrolyte membranes, and electrodes form an interdependent triad. Any inefficiency within one component can significantly compromise the overall performance of the flow cell. The operational success of OFB thus depends strongly on the interfacial contact quality and electron-transfer rate compatibility between the RAM and electrode surface. During operation, the electrolyte is circulated through high-surface-area porous electrodes that promote intimate contact with the redox species and enable electron transfer predominantly via the inner-sphere mechanism, which is preferred for efficient redox conversion. Various forms of carbon-based electrodes, such as carbon felt, carbon cloth, graphitic carbon paper, foams, and emerging 3D-printed structures, are widely employed due to their low cost, chemical stability, abundance, resistance to oxidative degradation, and versatile surface processability, which enhances wettability and electrochemical performance.

The physicochemical properties of carbon electrodes can be further optimised through surface modifications, including *in situ* electrocatalyst deposition, thermal

activation, oxidative treatments, or incorporation of catalytic additives. These treatments generate hierarchical micro and macroporous structures that improve mass transport, reduce pressure drop, and enhance energy efficiency by lowering activation overpotentials compared with pristine hydrophobic carbons. Ideally, the electrode material also suppresses unwanted electrochemical gas evolution by modulating the system's overpotential. In high-voltage flow cells (electromotive force > 1.5 V), undesired side reactions such as the Hydrogen Evolution Reaction (HER, $H_2\uparrow$) and Oxygen Evolution Reaction (OER, $O_2\uparrow$) can occur, leading to charge imbalance and efficiency losses over prolonged operation. Although OER proceeds more slowly than HER, electrode surface engineering effectively mitigates these parasitic processes, particularly the latter[30,31]. Ultimately, the performance and stability of OFB are dictated by the interplay between charge-transfer kinetics, cell conductivity, and concentration gradients of electroactive species near the electrode-electrolyte interface.

2.3 Performance Matrices to Determine the Competitiveness of OFB

The performance of an organic flow cell is assessed through several key parameters, including various efficiency metrics, overpotential, power density, area-specific resistance, capacity retention, maximum specific capacity, current density, and long-term cycling stability. Due to the diversity in RAM, PEM, electrode compositions, cell architectures, operating modes, and physicochemical environments, each OFB system exhibits distinct energy storage characteristics tailored to specific application demands[2,32,33]. This section outlines the principal performance descriptors governing OFB operation and proposes standard evaluation guidelines to ensure consistent and comparable assessment across different device configurations.

2.3.1 Efficiencies

The efficiency of an RFB is defined as its ability to deliver a specific amount of electrical energy during discharge relative to the energy consumed during charging, measured at equivalent states of charge for both processes. In FB, performance is commonly evaluated using three key efficiency parameters, namely, Coulombic Efficiency (CE), Voltage Efficiency (VE), and Energy Efficiency (EE), which together provide a comprehensive measure of electrochemical reversibility and the overall stability of the flow cell.

Coulombic Efficiency (CE): Coulombic efficiency is defined as the ratio of the discharge to charge capacities, or as the ratio of discharge time to charge time under a given applied current density.

$$CE = \frac{Q|discharge}{Q|charge} = \frac{\int I_{discharge} dt}{\int I_{charge} dt}$$

Voltage Efficiency (VE): Voltage efficiency is defined as the ratio of the average discharge voltage to the average charge voltage of a Redox Flow Battery (RFB) under a given applied current density. It represents the extent of voltage losses due to internal resistance, electrode polarisation, and mass-transport limitations within the cell.

$$VE = \frac{\int V_{discharge} dt}{\int V_{charge} dt}$$

Energy Efficiency (EE): Energy efficiency is defined as the ratio of the total electrical energy delivered during discharge to the electrical energy consumed during charging, measured at equivalent states of charge. It reflects the combined effects of electrochemical reversibility and voltage losses within the system.

$$EE = CE \times VE$$

In contrast to solid-state storage batteries, OFB are designed as grid-scale, sustainable energy storage systems and are often referred to as Virtual Energy Storage Systems (VSES) due to their modular and decoupled architecture. OFB constitute dynamic electrochemical assemblies that integrate several interdependent components like RAM, PEM, electrodes and flow circuits, each contributing to the entire cell performance. Beyond the commonly reported CE, VE and EE, another crucial but often overlooked parameter is the Round-Trip Efficiency (RTE), which accounts for both electrochemical and mechanical energy losses. RTE is defined as the ratio of the total electrical energy retrieved during discharge (net power output, P) to the total electrical energy supplied during charging, including ancillary losses such as pumping and flow circulation energy.

$$RTE = \frac{P|discharge}{P|charge}$$

Improving RTE requires simultaneous optimisation of all major components-RAM chemistry, membrane

selectivity, electrode architecture, flow field design, and operational parameters.

Furthermore, during cell operation, individual charge and discharge efficiencies can also be evaluated to quantify energy conversion effectiveness under practical working conditions simply from the square root of round-trip efficiencies as Battery Charge Efficiency (BCE) = Battery Discharge Efficiency (BDE) = RTE[5].

2.3.2 Overpotential in Flow Cell Operations

In an ideal OFB, there should be negligible ion or volume migration of the positive and negative electrolytes across the separator into the counter-electrolyte reservoirs. However, in practice, differences in concentration and electrochemical potential gradients induce polarisation within the cell through localised mass transfer at the electrolyte-membrane interface, an unavoidable phenomenon in redox flow cells during operations. In an electrochemical cell, the additional potential required to drive a redox reaction beyond its thermodynamically predicted value is termed the overpotential (η). Consequently, the total cell voltage and associated overpotentials can be categorised as (i) Open-circuit voltage (η_{OCV}), corresponding to the thermodynamic equilibrium potential; (ii) Activation overpotential (η_{act}), arising from charge-transfer kinetics at the electrode surface; (iii) Ohmic overpotential (η_{ohm}), due to resistance from ionic and electronic transport through the electrolyte, membrane, and electrode; and finally, (iv) concentration overpotential (η_{conc}), resulting from mass-transport limitations and concentration gradients during operation (Figure 4a).

Open-Circuit Voltage (OCV/OCP): The OCV represents the net Electromotive Force (EMF) of an electrochemical cell when no external current is applied between the electrodes, that is, under zero-current conditions. It corresponds to the thermodynamic equilibrium potential of the redox couple and excludes contributions from kinetic or transport-related overpotentials. Experimentally, deviations from the theoretical equilibrium potential may reflect residual η_{act}, η_{ohm}, or η_{conc} present even at near-equilibrium states (Figure 4b).

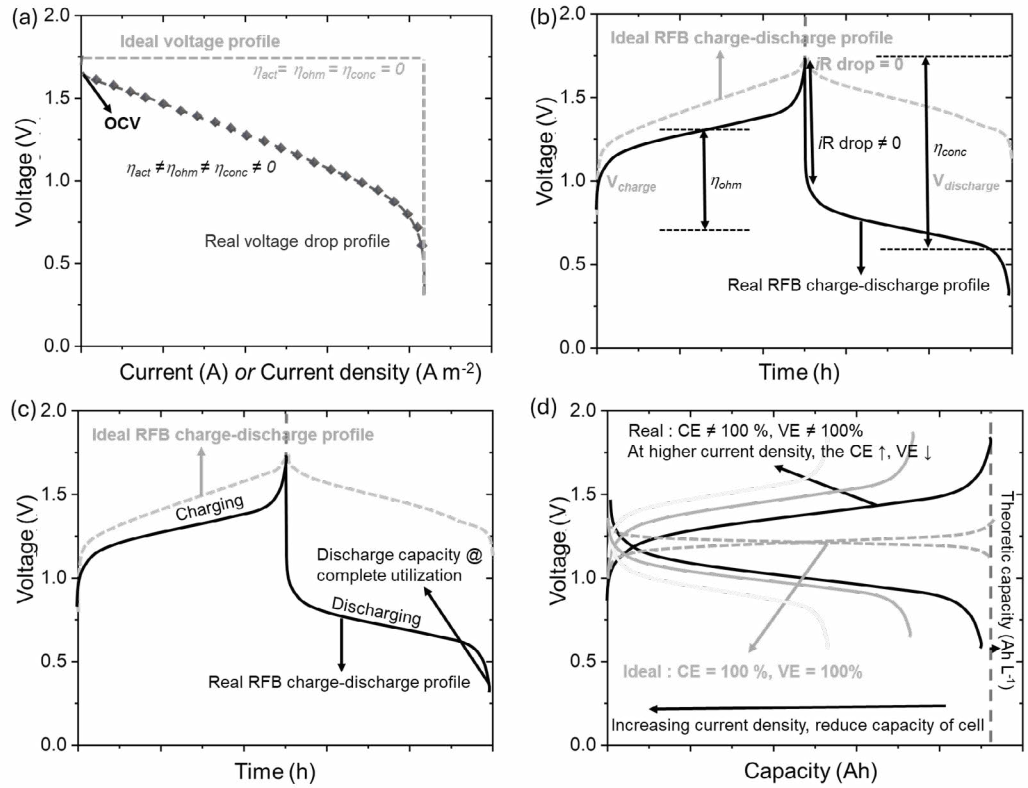


Figure 4. Schematics of different losses in OFB and Galvanostatic Charge-Discharge (GCD) profile and related parameters **(a)** Polarisation curve **(b, c)** GCD curve showing evaluation parameters and matrices and **(d)** GCD curve (voltage *vs* capacity plot, the α-curve) and influence on efficiencies/capacity with variable current density operations.

Activation Overpotential (η_{act}): The activation overpotential is the additional potential required to overcome the activation energy barrier associated with the charge-transfer process at the electrode-electrolyte interface. It represents the kinetic limitation of the redox reaction and determines the onset of measurable current generation in an organic flow cell. Lower η_{act} values indicate faster electron-transfer kinetics and superior electrocatalytic activity of the electrode material.

Ohmic Overpotential (η_{ohm}): Ohmic overpotential arises from the internal resistance to ionic and electronic conduction within the electrochemical cell. It follows Ohm's law, being directly proportional to the applied current and encompasses resistive losses originating from the electrodes, current collectors, PEM and the electrolyte itself. Minimising η_{ohm} is essential for improving voltage efficiency and overall energy conversion performance.

Concentration Overpotential (η_{conc}): Concentration overpotential results from the formation of concentration gradients between the electrode surface and the bulk electrolyte during operation. It becomes significant at high current densities, where mass-transport limitations hinder the diffusion of electroactive species to and from the electrode interface. In FBs, η_{conc} typically manifests near the cell's maximum capacity and contributes to polarisation losses under extreme operating conditions.

2.3.3 Capacity of a Battery and Related Profile Analysis

The capacity (Q) of a battery is defined as the total amount of electric charge that can be delivered during discharge at a nominal cell voltage for a given period. It represents the product of discharge current (in amperes) and time (in hours) and is expressed in ampere-hours (*i.e.*, Ah) (Figures 4c-4d). In RFB, capacity is primarily governed by the amount and concentration of electroactive species present in the electrolyte solution. The theoretical capacity (Q_{theor}) denotes the maximum possible charge that a flow battery can deliver under ideal electrochemical conversion conditions and is mathematically defined as Theoretical capacity

$$(Q_{theor}) = \frac{n[\text{RAM}]\times V_{eff}\times F}{3600}\ .$$

[*Note:* n = no. of transferable electrons per mole (≥ 1), [RAM] = concentration of redox active molecules (mol L^{-1}), V_{eff} = effective electrolyte volume in Liters (L) and F = Faraday's constant as 96,485 C mol^{-1})]. Whereas specific capacity (Q_{sp}, also *volumetric capacity*) of an FB is defined as the experimentally measured capacity (Q_{exp}) per unit volume of electrolyte (V_{eff}) and is expressed in Ampere-hours per litre (Ah L^{-1}). Specific or volumetric capacity $(Q_{sp}) = \frac{Q_{exp}}{V_{eff}}$

This parameter provides a direct measure of how efficiently the electrolyte stores and releases charge during cycling. The corresponding energy density of the flow cell can be derived from Q_{sp} and the average discharge voltage (Section 2.3.4).

Furthermore, during prolonged cycling, capacity fading is an intrinsic degradation process arising from side reactions, redox species crossover, or irreversible chemical transformations. The Capacity Fading Rate (ΔQ) quantifies the decay in performance of FB and can be calculated from the difference between the maximum experimental capacity in the first cycle (or 2nd cycle, considering activation) and the residual capacity after the n^{th} cycle, normalised to the total number of charge-discharge cycles.

$$\Delta Q = \frac{Q_{exp,\,max} - Q_{exp,\,n}}{\text{Total no. of. cycles(n)}} \text{ (in Ah per cycle).}$$

Monitoring ΔQ enables comparative evaluation of long-term cycling stability and electrochemical durability of flow battery systems.

2.3.4 Energy Density and Power Delivery

The energy density of a battery is defined as the amount of electrical energy that can be extracted from the system per unit volume of electrolyte, accounting for the combined volumes of the posolyte and negolyte. It reflects the total stored energy relative to the electrolyte inventory and is expressed in watt-hours per litre (Wh L^{-1}). For OFB, the energy density is calculated as the product of the nominal cell voltage and the specific (volumetric) capacity as: Energy density in Wh $L^{-1} = Q_{sp}$ x Nominal voltage (V). Whereas the power density of an RFB describes the instantaneous power output per unit active area of the membrane and provides a direct measure of the device's rate capability. It is obtained from the peak of the polarisation curve, where the voltage-current response reaches its maximum power point during galvanostatic operation. Power density is expressed in milliwatts per square centimetre (mW cm^{-2}) as;

$$\frac{\text{Maxium current drew(Amp)} \times \text{Sustained stable cell voltage(in V)}}{\text{Effective area of the membrane}(m^2)}$$

2.3.5 Capacity Factor and Levelised Cost of Storage (LCS)

The most significant techno-economic indicators for assessing the market penetration and long-duration storage potential of RFB are the capacity factor and the LCS, also referred to as the Levelised Cost of Electricity (LCOE). The capacity factor represents the proportion of time a battery actively supplies electricity within a 24-hour period, assuming one complete charge-discharge cycle per day.

$$\text{Capacity factor (\%)} = \frac{\text{Discharge duration per day}}{24} \times 100$$

For instance, if an OFB operates for 1 h per day, the capacity factor is 4.2%, whereas a high-performance system delivering energy for 6h per day achieves a capacity factor of 25%. Furthermore, the LCS quantifies the lifetime expenditure of an energy storage system normalised to the total amount of electricity delivered over its operational lifespan. Expressed in U.S. dollars per megawatt-hour ($ MWh^{-1}), it encompasses all major cost components, including capital investment, installation, auxiliary hardware, research and development, administrative overheads, and operational margins[34]. In OFB, the polyelectrolyte membrane and RAM are the two most critical components influencing lifetime performance, energy efficiency, and overall storage cost. Minimising LCS while maintaining high energy efficiency and cycling stability is essential for the commercial viability of OFB technologies in real-world grid applications.

3. Recent Advancements in OFB Performances *via* Functional Modifications of RAM

The development and optimisation of flow battery technologies are advancing at an exceptional pace to address global warming challenges and provide viable energy storage solutions for intermittent renewable sources. As discussed earlier, the performance of OFB is inherently influenced by the interplay among its key components, *i.e.*, the RAM, electrodes and the separators. This section summarises the most recent progress in both aqueous and non-aqueous OFB systems, with a particular focus on the functional modification of RAM (Figure 5) aimed at achieving high-performance, durable, and long-cycling devices.

3.1 Strategic Devising and Molecular Designs in Advanced Aqueous OFB

3.1.1 Quinone-based OFB

To date, the progress in AqOFBs appears more reliable and dynamic than that of NAOFB. This superiority arises from their higher electrolyte conductivity (>300 mS cm^{-1}), inherently benign and non-hazardous design, low volatility of water-based electrolytes, and overall low cost[35]. Moreover, the stability and electrochemical conductivity of polymer membranes in aqueous systems demonstrate significantly greater resilience, exhibiting up to ten orders of magnitude higher ionic mobility for protons, hydroxides, and other counter-ions compared to those in organic solvents (Figure 5b). Since the LCS in any redox flow system is largely governed by the electrolyte lifetime, the rational design of RAM remains critical. Consequently, the primary focus in OFB development centres on enhancing broad pH and chemical stability, cycling durability, energy density, and electron-transfer efficiency of RAM, while improving oxidative stability, selectivity, and ionic conductivity in PEM.

Among organic redox motifs, quinones represent the most widely investigated RAM family due to their ease of functional modification and applicability in both anolyte and catholyte compartments. However, their relatively low energy density remains a key limitation, constrained by the narrow electrochemical stability window of ≈1.23–1.30 V, beyond which parasitic gas-evolution reactions occur. Among various quinones, anthraquinone and its derivatives have been extensively studied for long-life OFB applications. Symons suggested that high-performance quinones could be realised by tuning the density of tethered hydrophilic groups containing oxygen or charged functionalities such as tetraalkylammonium, sulfonate, or ether moieties, which suppress dimerisation and simultaneously enhance redox reversibility[36].

In 2014, Huskinson *et al.*[11] developed a high-efficiency (≈95%) metal-free OFB using a 9,100-Anthraquinone-2,7-Disulphonic Acid (AQDS) anolyte paired with a Bromine (Br_2) catholyte and a FUMASEP® membrane. This pioneering system demonstrated a low-cost electrochemical energy storage configuration independent of transition-metal salts. To eliminate bromine toxicity and chemical-gradient imbalances, Yang *et al.* designed an all-quinone flow cell using AQDS as the negolyte and 1,2-Dihydrobenzoquinone-3,5-Disulfonic Acid (BQDSH) as the catholyte over 12 continuous cycles. The

device maintained stable faradaic efficiency, confirming the chemical robustness of the organic system[37].

To overcome the inherent energy-density limitations, Lin *et al.* developed a hybrid OFB (HyOFB) using 2,6-dihydroxyanthraquinone (2,6-DHAQ) as the negolyte and ferri/ferrocyanide ($Fe(CN)_6^{n-}$, n = 3, 4) as the catholyte. At 20°C and ≈100% State of Charge (SoC), the device achieved energy efficiencies above 80% at a current density of 0.1 Acm^{-2} and power densities of 0.4 Wcm^{-2}, which further increased to 0.68 Wcm^{-2} at 45°C[13]. In 2017, a similar group[14] presented a comprehensive study on universal quinone-based electrode materials, achieving over 3000 stable cycles. Whereas Pyrene-tetraone[4,5,9,10] electrodes demonstrated 96% capacity retention over 1500 cycles, highlighting the feasibility of long-life performance comparable to industry benchmarks.

Similarly, Wang *et al.* reported an OFB employing 2-hydroxy-3-carboxy-1,4-naphthoquinone (2,3-HCNQ) as the anolyte and $K_4Fe(CN)_6$ as the catholyte, achieving nearly 100% coulombic efficiency and a peak power density of 0.26 Wcm^{-2}. The introduction of an electron-withdrawing carboxyl group shifted the electrode potential negatively by ≈30 mV compared to pristine 2-Hydroxy-1, 4-Naphthoquinone (2-HNQ)[38]. A simple hydroxy-substituted quinone, 2,5-dihydroxy-1,4-benzoquinone, investigated by Yang *et al.*, demonstrated high cycling stability at 0.1 A cm^{-2} and delivered a peak power density of 0.3 W cm^{-2} with ≈99.9% capacity retention. Complementary *in silico* modelling of functionally tailored tetra-substituted quinones further identified structural motifs yielding enhanced solubility, stability, and reduced internal resistance[39].

For long calendar life applications, 4,4′-((9,10-anthraquinone-2,6-diyl)dioxy)dibutyrate (2,6-DBEAQ) and its 1,2- and 1,8-isomers demonstrated exceptional stability in all-hydrocarbon configurations, with only 5% annual capacity fading representing the lowest degradation rate among quinone-based RAMs to date[15]. A subsequent phosphate-functionalised quinone with improved solubility (0.75M versus 35mM in DBEAQ-based systems at pH 9) achieved an unprecedentedly low capacity fading rate of 0.014% per day[17].

In 2019, Schlemmer *et al.*[40] introduced an economically viable, bio-derived quinone 2-Methoxy-1,4-Hydroquinone (MHQ), synthesised from vanillin (lignin precursor), priced at an estimated US$ 4 kg^{-1}. The resulting OFB exhibited remarkable stability over eight months of operation, completing at least one full charge-discharge cycle daily. However, limited solubility and degradation in concentrated H_3PO_4 (> 0.5 M) hindered further scalability. Compared to simpler naphthoquinones, which suffer from lower solubility, reduced stability, and higher permeability, bislawsone dimers demonstrated improved performance under alkaline conditions and are emerging as promising negolyte materials for high-energy density OFB[41]. Overall, these trends underscore that strategic molecular design tailoring functional groups, charge distribution, and steric environment is pivotal to achieving durable and efficient quinone-based OFB. Depending on molecular compatibility, quinones can be deployed across a wide pH range. Several studies have reported advanced hydrophilic spacers such as Polyethylene Glycol (PEG), β-dimethyl carboxyl substituents, telechelic -SO_3H groups, and trimethylammonium-based linkers, all of which have been explored to optimise redox reversibility and solubility in high-performance quinone-based OFB[16,18,19,35,42-51].

3.1.2 Alloxazines, Phenazine, Phenothiazine, Phenoxazine and Alloxybenzene-based OFB

Alloxazines are specialised electroactive molecules that exhibit highly stable redox reversibility in OFB (Figures 5a-5d). These linear tricyclic compounds, derivatives of pteridine, are structural tautomers of isoalloxazine motifs found in the riboflavin backbone. During charge-discharge operation, the central aza-aromatic ring containing C=N functional groups undergoes redox transformations analogous to those of quinones, following a radical-free mechanism. Inspired by flavin-based cofactors and *de novo* condensation reactions of small organic molecules such as alloxan and o-phenylenediamine (and their derivatives) under mild acidic conditions, Lin *et al.*[52] developed a comprehensive library of alloxazine-based RAMs. The -COOH tethered variants exhibited an EMF of 1.2V and achieved >99% capacity retention per cycle. Subsequent studies by Chang *et al.*[51] also reported encouraging results for COOH-substituted alloxazine systems, though the cause of observed performance degradation was not identified. In aqueous media, however, alloxazines are prone to degradation *via* ring-opening hydrolysis at the sp^2 carbon of the amidic functionality. *In silico* investigations by Qian *et al.*[53] indicated that electrolyte imbalance during extended charge-discharge cycling is the primary cause of capacity decay. Their analysis comprehensively described the influence of activation and concentration

overpotentials, electro-osmotic transport, electrode porosity, and energy requirements in alloxazine-7/8-carboxylic acid || ferro/ferricyanide OFB models. Due to limited functionalisation versatility and restricted tuning of redox potential and stability through electron-donating substituents, only a few advanced alloxazine structures have been reported for OFB applications.

Analogous to alloxazines, the phenazine, phenothiazine, and phenoxazine families can also facilitate two-electron transfer processes through lone pairs located in the π-orbitals of N, S, and O atoms, respectively. These biologically inspired aromatic structures display high volumetric energy densities, molecular diversity, and solubility across broad pH ranges, yielding excellent long-term stabilities and capacity retention in OFB systems. In 2018, Hollas *et al.*[54] systematically evaluated substituted phenazine derivatives by calculating Gibbs free energy for Two-Electron Transfer (ΔG_{ET}), Gibbs Solvation Energy (ΔG_{sol}), and employing Continuum Solvation (COSMO) screening. Among the tested derivatives, 7,8-dihydroxyphenazine-2-sulfonic acid (DHPS, -1.05V vs Ag/AgCl) and 7,8-dihydroxyphenazine-2-carboxylic acid (DHPC, -1.13V vs Ag/AgCl) exhibited the highest cell voltages when coupled with ferro/ferricyanide (0.34V vs Ag/AgCl) catholytes. At a concentration of 1.4M DHPS, the flow battery showed an exceptional capacity fading rate below 0.01% per cycle and 0.1% per day. Park *et al.*[55] synthesised benzo[a]phenazine and its hydroxyl- and sulfonate-functionalised derivatives, Benzo[a]Phenazin-5-ol (HBP) and Benzo[a]Phenazine-5-ol Methane Sulfonate (BHPS), respectively. The incorporation of bulky aromatic rings and ionic substituents mitigated the issues of hydrolytic instability, slow diffusion kinetics, poor redox reversibility, and limited solubility. Compared to HBP, BHPS-based flow cells demonstrated superior performance in BHPS || $Fe(CN)_6$ configurations, achieving >99.5% CE and ≈99% capacity retention at 60 mA cm^{-2}. Kong *et al.*[56] reported a long-side-chain phenazine derivative, 4,4′-(phenazine-2,3-diylbis(oxy)) dibutyric acid, coupled with $Fe(CN)_6$-based catholytes. This device exhibited >99% capacity retention, a fading rate of 0.0127% per day at 20mA cm^{-2} for 1000 cycles, and CE >99.9%, with energy efficiency decreasing by only 4% after 40 days of operation. In a related study, Liu *et al.*[57] operated a similar architecture at a higher current density (50mA cm^{-2}), demonstrating stability over 1000 cycles.

Inspired by the S-doping effect observed in solid-state systems for enhancing redox potential, phenothiazine-based electrolytes were also explored. Zhang *et al.*[58] developed a methylene-blue-based symmetric organic flow cell exhibiting a high electron-transfer rate constant (0.32cm s^{-1}) and solubility up to 1.5M. The device delivered a reversible capacity of ≈71Ah L^{-1} without measurable fading over 1200 cycles at 80mA cm^{-2}, outperforming alloxazine-based cells of similar aromatic length[55,57]. Likewise, an oxygen analogue gallocyanine-KOH (2e^- RAM) was investigated by Martinez *et al.*[59]. This system achieved ≈100% CE and retained 87% capacity after 200 cycles at a low current density of 5mA cm^{-2}, highlighting that operational current density and energy density remain key challenges for phenoxazine-based flow batteries.

In a subsequent study, Fang *et al.*[60] introduced hydrophilic modifications *via* halato-telechelic trimethylammonium functionalization, enhancing solubility to 1.8M and enabling stable cycling for 200 cycles at 10mA cm^{-2} with a capacity fading rate of 0.16% per cycle. Despite these improvements, the modified N-(3-trimethylammoniumpropyl) phenoxazine chloride still exhibited precipitation issues, underscoring the need for further optimisation of solubility and molecular stability in phenoxazine-based redox systems.

3.1.3. Viologen-based OFB

Viologens, originally known as herbicidal compounds, possess a 4,4′-bipyridinium ring structure that undergoes reversible redox conversion to form a stable radical cation during electrochemical cycling (Figure 5e). These molecules have gained significant attention as two-electron RAM for OFB electrolytes. Attributed to their high aqueous solubility and excellent redox reversibility, viologens are extensively studied for high-energy-density storage applications. The classical paraquat (methyl viologen) and diquat scaffolds serve as principal motifs that can be rationally modified to improve solubility, electrochemical stability, and performance. Prior studies suggest that functionalisation of RAM with ionisable groups enhances electrochemical stability and energy efficiency compared to their pristine counterparts. In conventional viologens, solubility often decreases upon reduction; However, π-extended viologens with fused aromatic rings display improved voltage stability and enhanced electron mobility between electroactive centres through planar conjugation bridges[61]. Luo *et al.*[62] designed a π-conjugated, thiazolo[5,4-d]thiazole-bridged viologen, 4,4′-(thiazolo[5,4-d]thiazole-2,5-diyl)

bis(1-(3-(trimethylammonio)propyl)pyridin-1-ium) tetrachloride, which exhibited excellent water solubility and remarkable cycling stability. The reinforced thiazole backbone enabled 99.97% capacity retention per cycle and 70% Energy Efficiency (EE) at 100mA cm^{-2}. Similarly, Huang *et al.* explored di-alkyl diquat derivatives achieving solubilities above 2M, where near-planar structures stabilised by extended bridging frameworks afforded improved durability under flow conditions. To enhance redox performance, DeBruler *et al.*[63] synthesised cation-exchanging viologens bearing sulfonate groups with two and three-carbon linkers. The resulting system demonstrated an exceptional CE of 99.99% and EE ≈ 67% at 60mA cm^{-2}, supported by Density Functional Theory (DFT) studies showing that Donnan exclusion and size-selectivity favoured compatibility with cation-exchange membranes.

Replacing sulfonate with Tetramethylammonium (TMA) groups, Hu *et al.*[64] achieved further performance improvement, including a 27% increase in peak power density (123mW cm^{-2}) and superior capacity retention. Liu *et al.*[65] extended this approach, evaluating TMA and hydroxyl-terminated viologens. DFT calculations confirmed that substituting TMA with hydroxyl groups decreased the Highest Occupied Molecular Orbital-Lowest Unoccupied Molecular Orbital (HOMO-LUMO) energy gap, while elongation of alkyl chains further reduced band energies. The propyl-hydroxyl viologen exhibited the best solubility and stable cycling at 100mA cm^{-2}, delivering a power density of ≈100mW cm^{-2} at nearly 100% state of charge. Ohira *et al.*[65] introduced a multi-electron-transfer dendrimer-type viologen featuring a high net positive charge density; however, the scaffold suffered from limited electrochemical stability.

Another strategy to suppress viologen dimerisation and enhance structural resilience involved host–guest inclusion. Liu *et al.* encapsulated methyl viologen within α-Cyclodextrin (α-CD), reducing the capacity fading rate from 0.35% to 0.075% per cycle at full utilisation[67]. A detailed account of advanced viologen architectures developed up to 2021 was provided by Kathiresan *et al.*[68]. Building upon Liu's concept, Kurshunov *et al.* proposed supramolecular viologen assemblies[69,70]. Among these, the 1-decyl-1′-(3-(trimethylammonio) propyl)-4,4′-bipyridinium tribromide (ADV) displayed the highest volumetric energy density over 500 cycles, whereas the 1-decyl-1′-(2-(2-(2-methoxyethoxy)ethoxy) ethyl)-4,4′-bipyridinium dibromide (EDV) achieved superior capacity retention at an operational current density of 8.33mA cm^{-2} [69] Martinez *et al.*[71] investigated the effect of counter-ions on viologen decomposition and observed that Iodide (I^-) counter-ions suppressed dimerisation more effectively than hexafluorophosphate (PF_6^-). Another strategy to prolong OFB lifespan involved introducing steric constraints *via* rigid rod–coil side chains, which reduced intermolecular interactions and mitigated degradation. This study provided the first comparative stability analysis of rod–coil and sigmoidal-shaped viologens[72]. Following the concept of π-extension, Pan *et al.* reported a benzene-bridged viologen paired with Pyr-TEMPO, achieving a power density of ≈320mW cm^{-2} and excellent capacity retention over 1000 cycles at 40mA cm^{-2} [73]. Most recently, Nikumbe *et al.* explored a series of highly soluble, functionalized viologen derivatives: Sulfonic acid (Viologen-SO_3H), carboxylic acid (Viologen-COOH), tetramethylammonium (Viologen-N^+Me_3), and imidazolium (Viologen–$MeIm^+$) as anolytes for high current density aqueous OFB. The flow cell performance followed the order Viologen-SO_3H > Viologen-COOH > Viologen-N^+Me_3 > Viologen-$MeIm^+$, with CE ≈ 99% and EE ≈ 66% at 100mA cm^{-2} [74]. Collectively, studies on viologen functionalisation demonstrate that hydrophilic modification, steric rigidity, and structural extension can significantly enhance stability, solubility, and volumetric energy density in aqueous OFB[75-84].

3.1.4 Ferrocene-based OFB

Ferrocene (Fc), a metallocene sandwich compound, is extensively employed in both aqueous and non-aqueous OFB systems owing to its excellent intrinsic redox reversibility and high electrochemical stability (Figure 5f). Its relatively low production cost of approximately \$5-12 kg^{-1} further supports its feasibility for large-scale applications. However, Ferrocene (Fc) suffers from inherently poor solubility, necessitating the introduction of hydrophilic functional groups or host–guest strategies to enhance performance. Kim and Kim *et al.* reported a highly soluble (≈3 M) and electrochemically reversible ferrocene derivative, dimethyl ethyl ferrocenyl methylammonium bromide, though stable performance was demonstrated only for 20 cycles[85]. Zhao *et al.* investigated sulfonated ferrocene as a catholyte for pH-neutral OFBs and observed that ferrocene-1,1′-bis(sulfonate) undergoes decomposition via nucleophilic substitution in strong alkaline media but remains stable in less aggressive nitrate-based electrolytes[86]. Nevertheless,

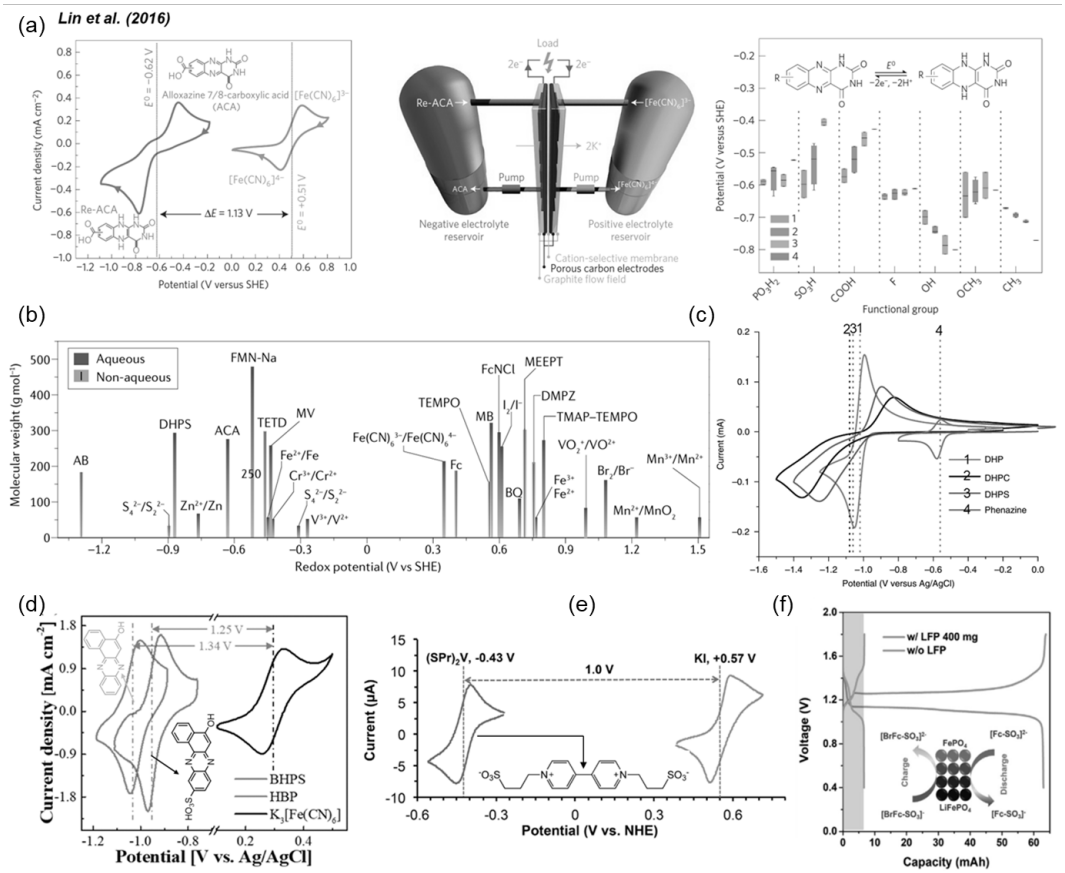


Figure 5. Recent advancements in aqueous OFB: **(a)** An alloxazine-based organic flow battery and the influence of electron donating and withdrawing groups on the redox potential of alloxazine RAM, **(b)** Comparison of various redox molecules and their electrochemical potential (electrochemical window profile), **(c)** Influence of cation exchange functional groups *viz* -COOH, -SO_3H and -OH groups on phenazine based RAM, **(d)** Cyclic voltammogram illustrating perturbations exhibited by sulfonic acid group on redox potential of hydroxy-phenazine, **(e)** 1V cell potential with sulfonated viologen and **(f)** Change in the charge-discharge specific capacity of Ferrocene based OFB with and without Li-based salt additive[52,54,55,63,87].

the cycling stability was inadequate for long-term operation, indicating the need for alternative molecular designs. To address the limitations of ferrocene-1,1′-bis(sulfonate) and trimethylammonium propyl substituted analogues, which exhibit poor compatibility with negatively charged Nafion® membranes, Yu *et al.* functionalised both cyclopentadienyl rings of ferrocene with sodium sulfonate propyl groups. The resulting system, benefiting from Donnan co-ion exclusion due to identical charge polarity, retained 99.9975% capacity over 1000 cycles at 80mA cm^{-2} [87]. Similarly, a comparable high-capacity retention (99.993% per hour) in anion-grafted ferrocene RAMs, confirming that extender chains of up to three carbon atoms represent an optimal design for such modifications[88]. To delineate the capacity fading, degradation mechanisms of Tetramethylammonium (TMA)-functionalised ferrocene were investigated by Luo *et al.* (Figure 6a), revealing that hydrolysis-induced ring detachment occurs under charged states[89]. To integrate both anionic and cationic functionalities, Zhang *et al.* developed zwitterionic ferrocene derivatives, though these also exhibited stability challenges during extended cycling[90]. Recent advancements in Fc-based RAM collectively underscore the importance of designing hydrolytically robust ferrocene derivatives to achieve ultra-long cycling stability and high energy density in both aqueous and non-aqueous OFB configurations[91,92].

3.1.5 TEMPO-based OFB

Recent advancements in the synthesis of stable organic molecules for negative electrolytes in aqueous OFBs are well established; however, only limited progress has

been made toward developing durable high-potential organic posolytes. The synthesis of hydrophilically tailored TEMPO derivatives represents a promising alternative to the previously discussed RAMs. Liu *et al.*[93] developed an ultra-stable aqueous OFB employing 4-[3-(trimethylammonio)propoxy]-2,2,6,6-tetramethylpiperidine-1-oxyl (TMAP-TEMPO) chloride as the catholyte, synthesised at an estimated cost of $6 kg^{-1} (Figure 6b). Operating at a cell voltage of 1.1 V, the device achieved excellent CE and stable capacity retention exceeding 99% over 1000 cycles at 40mA cm^{-2}, with aqueous solubility above 4.5M. Even at higher electrolyte concentrations, the cell remained operational, although slight efficiency and capacity losses were observed, likely due to chemical polarisation or decomposition processes.

Similarly, carboxylic acid–functionalised TEMPO-4-carboxy-2,2,6,6-tetramethylpiperidin-N-oxyl(4-COONa-TEMPO) and amine-functionalised analogues were investigated for long-term stability, showing capacity retention over 400 and 200 cycles, respectively[94,95]. Numerous subsequent studies have explored sulfonic acid substitutions, di-cationic motifs, and molecular size confinement strategies for TEMPO derivatives[79,80,96-99]. These reports collectively indicate that the functional modification trends in TEMPO-based systems mirror those established for quinone, viologen, and other organic RAM-based chemistries. Importantly, the cell potential and operational parameters remain unique to each RAM, necessitating systematic evaluation and screening according to industrial and Department of Energy performance standards. Furthermore, redox-active systems that integrate both n- and p-type functionalities (*i.e.*, bipolar RAM) are discussed in Section 3.3.

3.2 Recent Advances in Molecular Designs for Non-aqueous OFB

The high stability of organic supporting electrolytes and their broad electrochemical window constitute the principal advantages of NAOFB systems. However, the hazardous nature of organic solvents and their inherently low ionic conductivities often limit practical implementation, rendering aqueous OFB more favourable in most cases. Consequently, only a limited number of studies have reported discrete yet notable advances in molecular design and cell configuration for NAOFBs. In 2018, Chen *et al.* synthesised a series of seven viologen-based negolyte incorporating alkyl-chain extenders namely $-CH_3$, $-CH_2CH_3$, $-(CH_2)_2CH_3$, $-(CH_2)_5CH_3$, benzyl ($-CH_2Ph$), methylene-ester ($-CH_2COOCH_3$), and ether ($-CH_2OCH_3$) and evaluated their performance with bis(2,2′:6′,2″-terpyridine)iron(II) tetrafluoroborate as the catholyte[100]. Among the series, the six-carbon chain viologen exhibited the highest compatibility with carbonate-based electrolytes, achieving CE > 98% and EE > 84% over 20 cycles at a low current density of 0.5 mA cm^{-2}. Despite these encouraging metrics, the overall performance remained inferior to aqueous counterparts, highlighting the conductivity limitations of non-aqueous media. To improve voltage and stability, Kwon *et al.* developed a bio-inspired multi-redox organic catholyte, 5,10-bis(2-methoxyethyl)-5,10-dihydrophenazine (BMEPZ), paired with 9-Fluorenone (FL) as the anolyte, achieving a cell potential of 2.0V (10). The device demonstrated excellent stability with 99.94% capacity retention per cycle over 200 cycles at 20mA cm^{-2}. In a related effort, Chai *et al.* employed polyethene glycol-based micellar viologen architectures, wherein the large dendrimer-like morphology effectively suppressed crossover of electroactive species, maintaining ≈80% capacity retention at 2mA cm^{-2} [101].

Further exploration into triazenyl carbene-based N-heterocyclic carbene RAMs by Back *et al.*[102] and bis(pyridinylidene)-type two-electron transfer anolytes by Alkhayri *et al.*[92] yielded promising redox activity but suffered from poor cyclability and low efficiencies. Additionally, Giri and Dash provided a comprehensive review of ferrocene and TEMPO-based redox-active materials, outlining their relevance to both aqueous and non-aqueous systems.

Intriguingly, different organic molecules based on the new triazenyl-carbene-based N-heterocyclic carbene RAM were explored by Back *et al.* Further, a 2 e^- transfer bispyridinylidene-based anolyte was explored by Alkhayri *et al.* However, for both molecules, the major setback was low cyclability and low efficiency. Ferrocene and TEMPO-based electroactive materials were summarised and reviewed by Giri and Dash. Overall, literature on NAOFB indicates that achieving high performance requires addressing internal resistance through enhanced electrolyte conductivity, the integration of advanced membrane materials, and the rational design of novel electroactive molecules capable of stable operation across wide voltage ranges.

3.3 Advanced Bipolar and Polymeric Redoxmers OFB Cell Performances

Bipolar and polymeric redox-active electrolytes represent an emerging class of electroactive materials that integrate both n- and p-type functionalities within a single molecular framework, offering synergistic electrochemical advantages. Depending on the performance requirements of the OFB, these materials can be rationally tuned for both aqueous and non-aqueous systems. The use of bipolar RAM offers three principal advantages *viz* (i) Similar to all-vanadium or all-iron RFBs, a single molecule can serve simultaneously as both anolyte and catholyte, thereby eliminating cross-contamination-induced performance decay and enabling facile rebalancing without irreversible capacity loss, (ii) Enhanced molecular interactions with charged membranes, which improve interfacial contact and reduce overall cell resistance particularly in aqueous OFB, and (iii) Intrinsic mitigation of concentration gradients arising from differences in solubility and chemical structure[7,99,103]. To address the irreversible capacity losses and crossover-induced instabilities of conventional aqueous OFBs, Zhu *et al.*[104] designed an artificial bipolar molecule for pH-neutral systems consisting of a covalently linked ferrocene-viologen hybrid (Fc-bipy^{3+} trichloride). Computational and electrochemical analyses confirmed high redox stability and reversibility, yielding outstanding cycling performance with 75% capacity retention over 4000 cycles and CE > 99.8%. In a separate approach, Borchers *et al.*[105] synthesised a strategically tailored redox-active monomer polymerised with a quaternary ammonium containing halato-telechelic acrylate to produce a miscible redox polymer electrolyte for aqueous OFB operating at 60°C. The device exhibited CE > 99% and stable capacity retention over 100 cycles at 4mA cm^{-2} (Figure 6c). Similarly, Hagemann *et al.*[106] developed a polymeric redox-active electrolyte integrating the 2,2,6,6-tetramethylpiperidin-1-yl)oxyl (TEMPO) motif with a hydrophilic zwitterionic comonomer, [(2-(methacryloxy)ethyl)dimethyl-(3-sulfopropyl)] ammonium hydroxide, demonstrating the feasibility of polymer-based RFB.

Another innovative approach employed a bromide counter-ion based viologen, self-trapped *via* tribromide complexation to form MV_2, which exhibited intrinsic bipolar behaviour and effectively mitigated bromine gas evolution. The resulting near-symmetric 1.53 V MV/Br OFB achieved a peak power density of ≈135 mW cm^{-2} and ≈100% capacity retention, though the EE remained below 60% at 60mA cm^{-2}, indicating a need for further solubility (>1.5 M) and stability improvements[107]. A phenothiazine-based small bipolar molecule was subsequently designed for 2.5V OFB by Liu *et al*[108], achieving excellent cycling stability over 500 cycles at 10mA cm^{-2} with an average EE of 84%. In another notable development, Wang *et al.* introduced a TEMPO-viologen bipolar RAM, 1-(1-oxyl-2,2,6,6-tetramethylpiperidin-4-yl)-1′-(3-(trimethylammonio)propyl)-4,4′-bipyridinium trichloride, which exhibited superior efficiency at current densities six times higher than those used for phenothiazine-based bipolar systems[109]. Although bipolar and polymeric RAM display excellent efficiency, stability, and crossover resistance, their energy densities remain a key challenge. Continued efforts in molecular engineering are essential for advancing these next-generation electrolytes toward competitiveness with established inorganic flow battery chemistries.

4. Advancements in Polymer Electrolyte Membrane Designs for OFB

4.1 Cation Exchange Membranes (CEM)

Attributed to the high cation mobility and excellent bulk ion selectivity of CEM, aqueous OFB are most effectively assembled using dense polymer membranes functionalised with highly ionisable Sulfonate (-$SO_3^-M^+$) or Sulfonic acid (-SO_3H) groups. However, since no ion-exchange membrane exhibits absolute counter-ion selectivity, some degree of co-ion leakage is typically observed under high current density operation, which can adversely affect long-term OFB cycling stability and lifespan through electro-osmotic drag effects, particularly in fluorinated commercial membranes such as Nafion. In alignment with the Department of Energy (DoE) target of achieving a 90% cost reduction within the next decade, extensive efforts are being directed toward the design of low-cost hydrocarbon-based CEM as viable alternatives for OFB applications.

Among commercially available CEM, Nafion (Figure 7a) and Sulfonated Poly(Ether Ketone) (sPEEK) are the most widely utilised in OFB. In studies employing various RAM, Nafion-117 and Nafion-212 remain the standard benchmark separators. However, recent developments

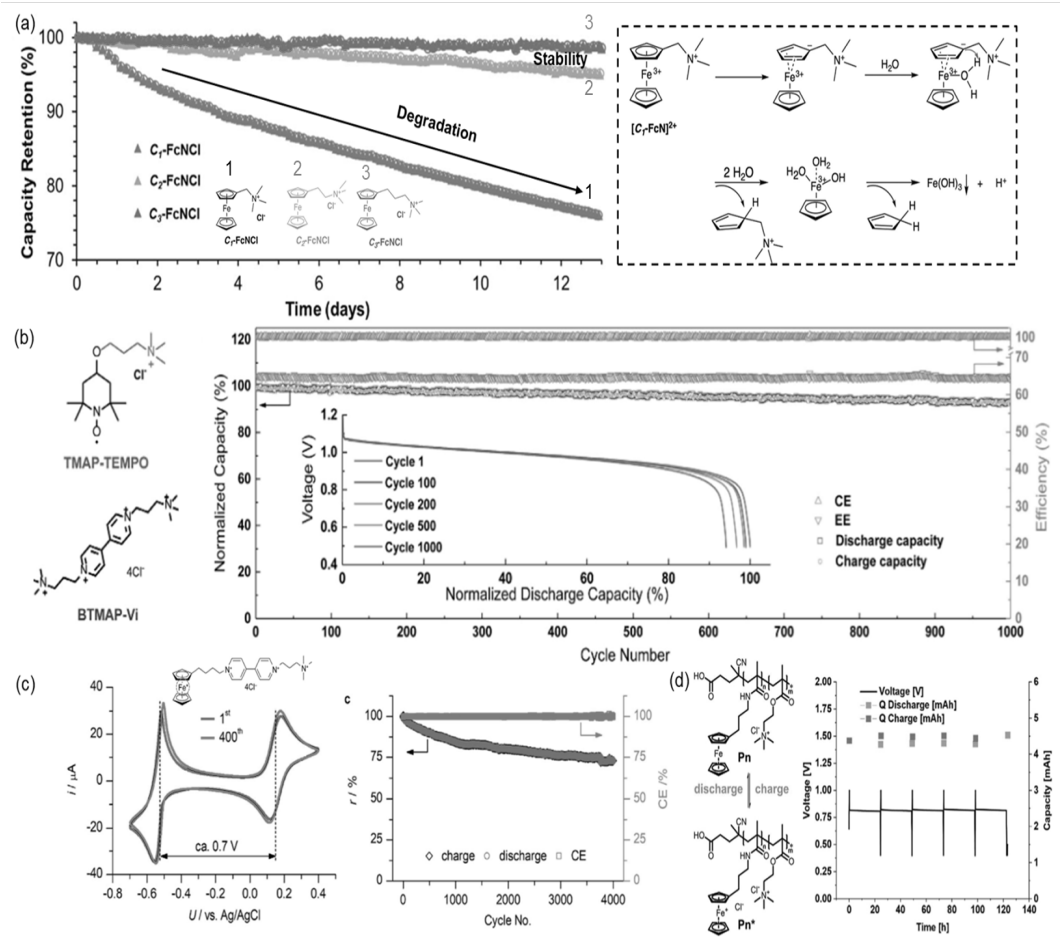


Figure 6. **(a)** Performance evaluation (long-cycling) of various ferrocene based electrolytes and the influence of side-chain on stabilities (showing degradation mechanism of pristine Ferrocene (CrFeNCl), **(b)** TEMPO-viologen based highly stable OFB device, **(c)** A bipolar organic electrolyte and its stability profiling with cyclic voltammogram for 1st and 400th cycle (assembled cell shows high capacity retention for 4000 cycles and **(d)** Redox active polymer and its pulsed charge-discharge stabilities[89,93,104,105].

exploiting dead-end hydrophilic-hydrophobic phase separation in hydrocarbon-based membranes where the percolating domain size is significantly smaller than that of Nafion have produced promising results. For instance, Porcellinis *et al.*[110] investigated moderately sulfonated sPEEK membranes exhibiting negligible water transport (*i.e.*, no electro-osmotic drag) in a quinone (DHAQ) || $Fe(CN)_6$-based OFB operating at 250mA cm^{-2}.

Comparative performance analysis revealed minimal capacity loss (0.018% per cycle) and ionic conductivity ≈10mS cm^{-1} for sPEEK, whereas Nafion-212 exhibited 0.038% capacity loss and ionic conductivity of 6mS cm^{-1}, respectively. This study highlights that the reliance on costly fluorinated membranes such as Nafion can be substantially reduced by adopting speciality hydrocarbon-based polymers, including sulfonated poly(ether sulfone) and poly(phenylene ether), which offer comparable or superior ionic transport characteristics and enhanced economic viability for large-scale OFB deployment.

Similarly, Zhang *et al.*[111] investigated sPEEK membranes in 2,5-dihydroxybenzene-3,5-disulfonic acid/anthraquinone-2-sulfonic acid organic flow batteries. At an operational current density of 100mA cm^{-2}, the sPEEK membrane exhibited approximately 2% higher voltage efficiency compared to Nafion, while achieving a reversible capacity of ≈97% after 100 charge–discharge cycles. Demonstrating the competitive performance of polyarylene-based CEMs, Li *et al.* developed a sulfonated Poly(Phenylene Oxide) (sPPO) membrane for a $K_4[Fe(CN)_4]$/DHAQ aqueous organic flow battery operating at pH 14[112]. The negatively charged polymer

matrix enhanced stability, delivering 99% capacity retention and 81% energy efficiency over 500 cycles. A comparative structural analysis between sPEEK and sPPO (Figure 7a) revealed that the electron-withdrawing carbonyl groups in sPEEK are likely responsible for its relatively lower durability, owing to the electronegativity contrast between the carbonyl (in sPEEK) and ether (in sPPO) functionalities.

To further promote Donnan exclusion and suppress co-ion crossover, dual-ionic membranes bearing both cationic and anionic sites have been explored. Such architectures provide synergistic enhancements in ionic conductivity, facilitating concurrent cation and anion transport, while forming compact ionic networks that minimise active species loss. Drawing inspiration from salt-bridge and hydrogen-bond interactions in biological systems, Wang *et al.*[113] designed a Polymer of Intrinsic Microporosity (PIM) incorporating amidoxime (60 mol%) and carboxylic acid (40 mol%) moieties termed AO-PIM60% | cPIM40% for a phosphoric acid-based anthraquinone || $K_4[Fe(CN)_6]$ OFB (Figure 7c). The membrane demonstrated exceptional stability, maintaining performance for >2000 cycles at 80mA cm^{-2}, attributed to its high selectivity for monovalent ions in the supporting electrolyte. These results underline the potential of densified, ionically interactive polymer frameworks for advanced OFB membrane architectures. Tailoring polymer backbones for application specificity remains equally critical. A sulfonated anthrone-containing poly(aryl ether ketone) membrane was developed by Zhang *et al.* for a viologen^{++}-$(CH_2)_3$–SO_3H || $Fe(CN)_6$ pH-neutral OFB[114]. The system exhibited 97% reversible capacity and excellent long-term cycling stability for ≈3000 cycles, confirming the potential of high-performance thermosetting polymeric separators in durable energy storage applications. To overcome the alkali instability of conventional aryl-oxy bonds, Robb and George *et al.* designed sulfonated Diels-Alder polyphenylene membranes incorporating hydrophobic pentafluoroaryl shell architectures[115]. This core-shell-type structure enabled an exceptional peak power density of 1.23W cm^{-2}, complete crossover suppression at 100mA cm^{-2}, and minimal capacity loss of 0.02% per day, establishing a promising route toward commercially scalable OFB installations.

Analogous to dual-ionic designs, bi-functional membranes with strongly interactive ionic domains have also demonstrated superior performance. Sharma *et al.*[26] investigated the influence of sulfonation degree in poly(phenylene ether)-based membranes, further functionalized with bis-piperidinium-terminated graphene oxide for enhanced efficiency and durability in anthrarufin alkaline redox flow batteries (Figure 7d). The resulting bi-functional architecture, integrating optimised ionic microdomains and intercalated nanofillers, achieved >500-cycle stability under dynamic current switching up to 40mA cm^{-2}, delivering a peak power density of 88mW cm^{-2} with only 25mM redox electrolyte. The membrane retained ≈80% energy efficiency, demonstrating that substituting anthrarufin with more soluble RAM could further enhance OFB performance. Overall, these findings emphasise that advanced membrane fabrication strategies, including gradient sulfonation, bi-functional polyelectrolytes, ionically interactive polymeric frameworks, and high-density hydrocarbon architectures, represent viable pathways to achieve the desired balance between selectivity, conductivity, and stability for next-generation organic electrochemical energy storage systems.

4.2 Anion Exchange Membranes (AEM)

Assembling electrochemical cells with AEM (Figure 7b) can also serve as a viable approach in OFB. However, the chemical stability of polymer backbones and anion-conducting quaternary ammonium groups remains a challenge, particularly under alkaline conditions, where degradation and dealkylation of quaternary nitrogen sites compromise longevity. Conversely, under acidic environments, the limited anion conductivity of AEMs often results in reduced overall cell efficiency and energy density.

Using a poly(phenylene oxide) backbone, Li *et al.*[112] developed a chemically robust AEM incorporating trimethylammonium functionalities for TEMPO and viologen-based OFBs. The well-optimised ionic framework enabled the cell to exhibit cycling durability over 800 cycles, achieving ≈100mW cm^{-2} of power density at 40mA cm^{-2}. Moreover, the projected material cost below $\$10m^{-2}$ suggests significant potential for industrial-scale implementation of such membranes. To further address the issue of in situ degradation, Hou *et al.*[116] designed a self-healing membrane for pH-neutral OFB, based on a reversible Diels-Alder crosslinked network. The dynamic covalent crosslinks facilitated self-repair during electrochemical operation, thereby improving mechanical and chemical resilience. Although the membrane demonstrated promising efficiency performance, the power output was somewhat limited,

likely due to restricted ionic conductivity relative to conventional uncrosslinked AEM or sulfonated PEM.

Additionally, Tsehaye *et al.* synthesised a crosslinked poly(phenylene oxide)-based AEM incorporating a spirocyclic anion-exchange framework to achieve higher power delivery and durability in OFB applications[117]. These findings collectively indicate that crosslinking-based stabilisation and molecular architecture control in AEM can effectively extend their operational lifetimes and enhance electrochemical performance in next-generation organic flow battery systems.

Owing to their rigid and puckered molecular architectures, these membranes effectively suppress β-hydride elimination, rendering them suitable for high-pH alkaline flow battery applications[118]. To further enhance electrochemical conductivity, the incorporation of long-side-chain architectures, analogous to those in Nafion, combined with simultaneous crosslinking, has been widely explored. The extended chain length in such crosslinked frameworks promotes favourable nanophase miscibility and well-defined hydrophilic–hydrophobic domain separation, both of which are critical for efficient ion transport in electrochemical energy storage system[119]. Building on this principle, in Tsehaye's subsequent work, membranes incorporating a DABCO-based crosslinker and telechelic trimethylammonium groups demonstrated power densities of 300 mW cm^{-2} and energy efficiencies of 80%, respectively. Similarly, Peng *et al.* developed a new class of hyper-crosslinked AEM derived from trimethylammonium-functionalised poly(phenylene oxide) using dichloromethane as a room-temperature immersion crosslinking agent. This design enhanced ion selectivity by an order of magnitude, achieving conductivity up to 23mS cm^{-1}, surpassing both commercial AEM and polymers of intrinsic microporosity[77]. When compared with pristine, uncrosslinked membranes, these hyper-crosslinked structures exhibited ≈100% capacity retention (CFR = 0.0017% per cycle) over 400 cycles at 100mA cm^{-2}, while sustaining peak power densities of ≈302mW cm^{-2}. Recently, fluorinated polymer membranes based on Poly(Vinylidene Fluoride) (PVDF) and its hexafluoropropylene copolymer have also demonstrated promising electrochemical performance in aqueous pH-neutral OFB[120,121]. However, their application under alkaline conditions remains limited due to the high susceptibility of C-F bonds to dehydrofluorination, making these fluoropolymers more suitable for acidic vanadium RFB[122,123].

For instance, Sreenath *et al.* designed a high cationic charge density fluorinated membrane *via* O-nucleophile induced grafting of phenolic triamines onto PVDF-*co*-hexafluoropropylene, achieving high efficiency and cycling stability at 20mA cm^{-2}, suggesting suitability for low-pH and neutral-pH OFB[120]. Likewise, Shukla *et al.* employed a click-chemistry-mediated synthetic approach to produce membranes with improved ionic conductivity, highlighting their potential for aqueous organic electrochemical energy storage[121]. To further improve selectivity and chemical stability, Liu *et al.* introduced conformationally rigid Tröger's base frameworks[124], while microporous and ultramicroporous membranes prepared via superacid polycondensation[125] demonstrated promising ion-transport and mechanical properties. Evidently, these emerging architectures present valuable opportunities for the large-scale implementation of advanced AEM in OFB technologies.

4.3 Bipolar Ion-exchange Membranes

Bipolar ion-exchange membranes are a specialised class of membranes in which cation and anion-exchange layers are joined at an interfacial junction to form an n/p-interface. Only a limited number of studies have explored their application in OFB. One viable approach to increasing the cell voltage of an OFB involves replacing conventional unipolar membranes with bipolar counterparts. These bipolar membranes facilitate interfacial water dissociation, generating a pH gradient that can elevate the overall cell voltage[126]. Yan *et al.* incorporated a bipolar membrane into an OFB employing a sulfonate propyl viologen || $Fe(CN)_6$ redox couple. The bipolar configuration increased the cell voltage from ≈0.9 V to ≈1.6 V (≈44% enhancement), demonstrating a promising strategy to augment the energy-storage capacity of aqueous OFB[127]. Although most reported bipolar membranes are designed for acid-base redox flow systems, there are no known studies demonstrating their use with organic redox electrolytes. This absence is likely due to interfacial heterogeneity at the junction, which increases membrane resistance and can impair battery performance compared with conventional cation or anion-exchange membranes. Nevertheless, systematic investigations into the physical and electrochemical behaviour of such bipolar structures could provide valuable insights for expanding the operational voltage window of OFB and improving their overall energy efficiency.

4.4 Separators for Non-aqueous OFB

For non-aqueous OFB, where the supporting medium is an organic solvent, ion-exchange membranes are generally not preferred due to their limited chemical stability and high susceptibility to swelling or degradation in nonpolar environments. Consequently, separators with intrinsic porosity or engineered porous architectures capable of facilitating selective ion permeation while effectively suppressing crossover of organic molecules have been extensively investigated. Attributed to its excellent solvent resistance and low cost, polyethene has emerged as a common separator material; for instance, Wei *et al.*[128] utilised a porous polyethylene separator to evaluate a ferrocene-based non-aqueous OFB. Similarly, Celgard® 3501 (polyethene-polypropylene tri-layer composite) and Daramic® porous polyethylene separators are frequently employed for testing non-aqueous OFB systems[129-131]. In recent years, highly crosslinked ion-exchange membranes have gained attention as both self-standing membranes and pore-filled separator composites. Kim *et al.* developed a 25µm thick pore-filled anion-exchange membrane based on a crosslinked network of trimethylammonium methyl styrene and divinylbenzene[132]. The membrane demonstrated superior efficiency performance 87% in the stationary mode and 78% under flow conditions.

Similarly, Li *et al.*[133] fabricated a polyphenylene oxide-bipyridinium anion-exchange membrane, while Peltier *et al.* synthesised metathesis-polymerised (Grubbs' II catalyst) anion-exchange membranes with all carbon-carbon backbones for viologen || ferrocene-based non-aqueous OFB[134]. These membranes exhibited benchmark performance, retaining ≈80% capacity over 1000 cycles and maintaining an energy efficiency of 97%, with electrolyte crossover below 1% during charge-discharge cycling, demonstrating their strong potential for all OFB applications. In another study, Small *et al.* investigated Diels-Alder anion-exchange polymer membranes featuring hyper-knitted architectures in ionic-liquid-based non-aqueous OFB. The membranes achieved CE > 98%, high ion-exchange capacities (2.0meq g^{-1}), and excellent chemical stability, although their long-term mechanical stability remains to be fully assessed[135]. Based on these reports, it is evident that the development of crosslinked and composite polymer membranes represents a strategic direction for advancing membrane fabrication, offering a feasible pathway to replace conventional porous separators in next-generation non-aqueous OFB[136].

5. Modification of Electrodes for Improving OFB Performance

In RFB, particularly in the case of OFB, the electrode and the RAM are closely coupled components. However, they serve distinct functions. The electrode provides a conductive interface for electron transfer, while the redox-active species in the electrolyte store and release energy through reversible redox reactions. Since the

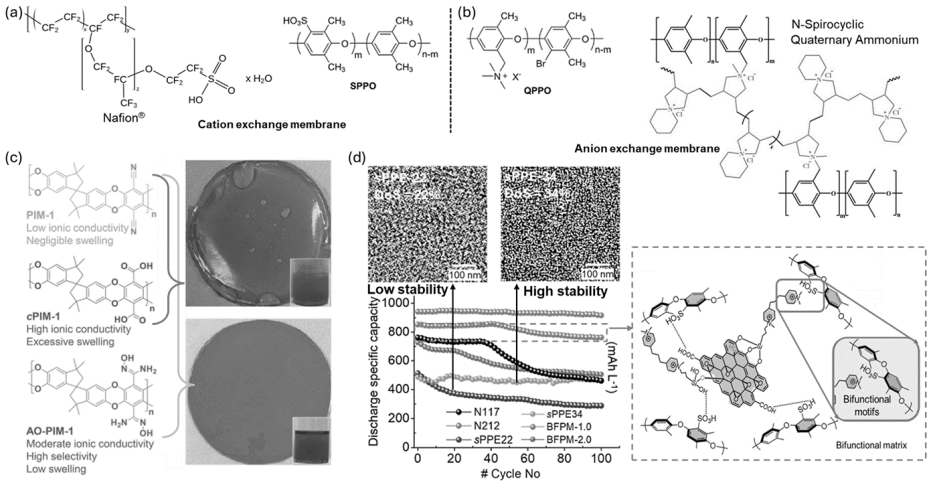


Figure 7. Recent advancements in polymer electrolyte membrane designs **(a)** benchmark Nafion, **(b)** hydrocarbon-based cation and anion exchange from poly(phenylene oxide), **(c)** polymers of intrinsic microporosity with acid-base interactions and **(d)** bifunctional polymer membrane and the influence of Degree of Sulfonation (DoS) on capacity retention profile[26,112,113,117].

redox reactions of organic molecules predominantly proceed *via* an outer-sphere mechanism, the electrode-electrolyte interfacial interaction is a critical determinant of performance[137]. Accordingly, graphite electrodes and their surface or bulk modifications can significantly enhance cell efficiency by reducing overpotentials and minimising interfacial resistance between the electrode, electrolyte, and membrane.

Depending on the electrolyte type and compatibility in OFB, electrodes may be optimised through intrinsic surface modification, electrocatalyst deposition, or surface-area enhancement. Among these, intrinsic modification achieved by increasing electrode hydrophilicity or functional tethering is particularly promising. Oxidative treatment of the carbon surface introduces ionic functionalities such as hydroxyl, carboxyl, and epoxide groups, thereby improving interfacial wetting and facilitating faster redox kinetics and higher electrolyte utilisation per cycle. For instance, Lee *et al.* developed an alloxazine-based OFB employing graphite felt modified with carboxylic acid functionalised carbon nanotubes[138]. The modified electrode enhanced the mass transfer of redox-active molecules and increased electron-transfer rates for organic electrolytes, while the kinetics for inorganic electrolytes (*e.g.*, ferro-/ferricyanide) remained largely unchanged. These results demonstrate that surface functionalities play a decisive role in governing redox reversibility, suggesting that donor-acceptor surface interactions can be a cost-effective route to improve OFB performance.

Further improvements can be achieved through heteroatom doping with elements such as N, S, or transition metals (*e.g.,* Fe, Co, Ni), which modulate surface electronic structure and catalytic activity. Gao *et al.* reported that pretreatment of rayon-based graphite electrodes enhanced the redox reversibility of the system. Additionally, the nature of dopant species influences reaction kinetics. For example, the peak separation of 1,8-dihydroxyanthraquinone redox couples followed the order Ni@graphite < Co@graphite < Fe@graphite, indicating more favourable kinetics for Ni-doped electrodes. Moreover, the position of hydroxyl substituents in the parent quinone was shown to affect flow-cell performance[139,140]. Chemical treatments and etching techniques can further increase surface area and introduce functional sites, although these methods have been more extensively studied in IFB. Recent reports have highlighted the potential of transient tailored wettability using D-fructose modification, wherein the high density of free hydroxyl groups generates oxygen-rich defect sites that improve electrolyte interaction for both organic and inorganic systems[141,142]. Overall, electrode modification strategies-including surface functionalisation, heteroatom doping, and wettability tuning-represent powerful approaches to enhance the energy efficiency and energy density of OFB.

6. Commercial Organic Flow Batteries

Recent technological evolution and industrial initiatives across Europe have significantly advanced the commercialisation of aqueous OFB, marking a transition from laboratory-scale prototypes to grid-connected energy storage systems. In contrast, non-aqueous OFB have yet to achieve comparable acceptance due to their demanding operational conditions, higher system complexity, and safety concerns associated with flammable or toxic organic solvents, factors that make aqueous systems more favourable for large-scale deployment. In 2020, JenaBatteries GmbH (Germany), in collaboration with BASF SE, successfully demonstrated one of the first industrial-scale OFB installations based on a TEMPO || methyl viologen redox couple, employing FUMASEP® ion-exchange membranes. The system achieved an energy storage capacity exceeding 100 kWh, with scalable modules projected to reach 400 kWh and beyond.

Similarly, KEMIWATT (France) developed commercial aqueous OFB systems operating at 10kW and 20kW capacities, utilising anthraquinone and ferro/ferricyanide redox pairs in conjunction with Nafion® polyelectrolyte membranes. Another European venture, Green Energy Storage (GES) (Italy), has engineered grid-level OFB prototypes based on sulfonated anthraquinone-bromine chemistries, also employing Nafion® membranes as the separator. These efforts collectively demonstrate the growing industrial confidence in aqueous OFB technologies as viable, sustainable, and modular solutions for medium- to large-scale stationary energy storage[143].

7. Challenges and Prospects on New Materials Design for Technology Propagation

Recent advancements in OFB technology have yielded significant insights into the design, performance, and

engineering of redox-active electrolytes, membranes, electrodes, and complete cell assemblies. The principal advantages of this emerging technology include the high processability of organic electrolyte materials, excellent cycling stability, broad molecular tunability of RAM for enhanced energy density, and inherently benign operating conditions. Benchmark studies using viologen, quinone, and TEMPO-based electrolytes have demonstrated months-long operational durability at high current densities, comparable to advanced inorganic flow batteries. Moreover, peak power densities exceeding 500mW cm^{-2} underscore the promising progress of OFB toward practical, grid-scale electrochemical energy storage. Based on the cumulative progress achieved to date, the transition of OFB from bench-scale research to industrial implementation appears both technically feasible and economically sustainable. A holistic understanding of the interactions among RAM, membranes, and electrodes will be pivotal in realising efficient and durable device chemistries. The following key directions summarise the current challenges and prospects for OFB technology.

(i) Enhancing solubility and redox reversibility of organic electrolytes: To achieve energy densities comparable to inorganic flow batteries, further efforts must focus on improving the solubility and redox reversibility of organic molecules in both anolyte and catholyte reservoirs. Increasing molecular hydrophilicity remains a promising route to achieving solubilities exceeding 2.5M. This can be achieved by introducing dissociable or polar functional groups such as $-SO_3H$, $-N^+R_3$, or extended alkyl spacers, or by strategically designing bipolar RAM. Insights into degradation pathways, including parasitic dimerisation, nucleophilic ring opening, and gas evolution (H_2 and O_2), reveal that these processes lead to electrolyte imbalance and capacity decay under high current densities. Therefore, simultaneous optimisation of solubility and molecular crowding represents a rational approach to mitigate these degradation-induced losses.

(ii) Rational membrane selection for aqueous and non-aqueous systems: The choice of membrane or separator material is crucial for stable and efficient operation. In aqueous OFB, advanced hydrocarbon-based polymer electrolyte membranes have demonstrated superior ionic conductivity and long-term durability compared to fluorinated counterparts. Conversely, polyethene-based porous separators have shown good stability in non-aqueous systems but often suffer from increased resistance and crossover losses. Promising future directions include the development of anion-exchange membranes devoid of aryl-oxy linkages, which could potentially offer enhanced chemical robustness, higher energy efficiency, and greater peak power density than current inorganic analogues.

(iii) Engineering electrode surfaces for improved redox kinetics: Carbon-based electrodes serve as the primary platform for rapid redox conversion in OFB. Hence, optimising their surface area, porosity, chemical functionalities, and wettability, particularly in non-aqueous systems, is essential. Gas-evolution reactions ($H_2\uparrow$ and $O_2\uparrow$) and other parasitic reactions, which can occur at elevated cell voltages, detrimentally affect efficiency and long-term stability. Thus, tailoring electrode surfaces through activation, doping, or catalytic modification can suppress these side reactions while enhancing electron transfer kinetics and electrolyte accessibility.

(iv) Establishing standardised evaluation protocols: Despite numerous reports on OFB performance, direct comparisons remain challenging due to the lack of standardised testing methodologies. Some studies emphasise energy or voltage efficiency, while others focus on capacity retention or cycle life at varying current densities. To ensure reproducible benchmarking, standardised experimental protocols are urgently needed. These should integrate metrics such as coulombic and energy efficiencies, operating current density, RAM stability, electrochemical kinetics, and long-term capacity retention evaluated under demand-specific operating modes relevant to practical energy storage applications.

8. Conclusion

Evidently, Organic flow batteries represent a sustainable, safe, and economically viable alternative to both conventional solid-state batteries and transition-metal-based flow systems, offering scalability from the megawatt-hour to terawatt-hour level. Their long operational lifetimes and exceptional potential for component modification open vast opportunities for

terrestrial deployment. Significant investments across Europe are already accelerating this technology, with global market expansion anticipated by 2050. Moreover, recent progress in the molecular design of organic redox-active materials, advanced membrane fabrication, and electrode surface engineering has contributed to steady improvements in energy efficiency, cyclability, and system durability. Nevertheless, the absence of standardised testing protocols and cross-comparable performance metrics continues to obscure a comprehensive understanding of device performance.

Among emerging chemistries, aqueous OFB are particularly promising for achieving large-scale, sustainable energy storage solutions. Beyond the discovery of new redox molecules and membrane materials, establishing a well-matched membrane-electrolyte interface capable of minimising internal resistance and enhancing electrochemical reversibility remains a central challenge. While certain aspects of this technology are still under exploration, OFB are widely regarded as a pivotal contributor toward the realisation of global sustainable energy storage goals in the coming decades.

9. Acknowledgement

J.S. gratefully acknowledges Dr Huacheng Zhang (Assoc. Prof., RMIT University, Melbourne) for her constant guidance, supervision, and invaluable support throughout the completion of this work. J.S. acknowledge financial support from the University Grants Commission (UGC), New Delhi, for UGC-JRF/SRF, File No. 191620048179 and the Royal Melbourne Institute of Technology (RMIT) University, Melbourne, for the RMIT-India Travel Fellowship Scheme (RITTFS) Scholarship.

10. References

1. Kim KJ, Park M-S, Kim Y-J, Kim JH, Dou SX, Skyllas-Kazacos M. A technology review of electrodes and reaction mechanisms in vanadium redox flow batteries. J Mater Chem A. 2015; 3(33):16913-16933. https://doi.org/10.1039/C5TA02613J
2. Zhang L, Feng R, Wang W, Yu G. Emerging chemistries and molecular designs for flow batteries. Nat Rev Chem. 2022; 6(8):524-543. https://doi.org/10.1038/s41570-022-00394-6 PMid:37118006.
3. Ding Y, Li Y, Yu G. Exploring bio-inspired quinone-based organic redox flow batteries: A combined experimental and computational study. Chem. 2016; 1(5):790-801. https://doi.org/10.1016/j.chempr.2016.09.004
4. Ding Y, Zhang C, Zhang L, Zhou Y, Yu G. Molecular engineering of organic electroactive materials for redox flow batteries. Chem Soc Rev. 2018; 47(1):69-103. https://doi.org/10.1039/C7CS00569E PMid: 29044260.
5. Soloveichik GL. Flow batteries: Current status and trends. Chem Rev. 2015; 115(20):11533-11558. https://doi.org/10.1021/cr500720t PMid:26389560.
6. Pan M, Shao M, Jin Z. Development of organic redox-active materials in aqueous flow batteries: Current strategies and future perspectives. Smart Mat. 2023; 4(4):e1198. https://doi.org/10.1002/smm2.1198
7. Sikukuu Nambafu G. Organic molecules as bifunctional electroactive materials for symmetric redox flow batteries: A mini review. Electrochem Commun. 2021; 127:107052. https://doi.org/10.1016/j.elecom.2021.107052
8. Ye C, Wang A, Breakwell C, Tan R, Grazia Bezzu C, Hunter-Sellars E, *et al.* Development of efficient aqueous organic redox flow batteries using ion-sieving sulfonated polymer membranes. Nat Commun. 2022; 13(1):3184. https://doi.org/10.1038/s41467-022-30943-y PMid:35676263 PMCid: PMC9177609
9. Catherine LP, Graham NN, Darren AW. Charge carriers for next-generation redox flow batteries. In: Olivier F, editor. Redox Chemistry. Rijeka: IntechOpen; 2022.
10. Kwon G, Lee K, Lee MH, Lee B, Lee S, Jung S-K, *et al.* Bio-inspired molecular redesign of a multi-redox catholyte for high-energy non-aqueous organic redox flow batteries. Chem. 2019; 5(10):2642-2656. https://doi.org/10.1016/j.chempr.2019.07.006
11. Huskinson B, Marshak MP, Suh C, Er S, Gerhardt MR, Galvin CJ, *et al.* A metal-free organic-inorganic aqueous flow battery. Nature. 2014; 505(7482):195-198. https://doi.org/10.1038/nature12909 PMid:24402280
12. Yang B, Hoober-Burkhardt L, Wang F, Surya Prakash GK, Narayanan SR. An inexpensive aqueous flow battery for large-scale electrical energy storage based on water-soluble organic redox couples. J Electrochem Soc. 2014; 161(9):A1371. https://doi.org/10.1149/2.1001409jes
13. Lin K, Chen Q, Gerhardt MR, Tong L, Kim SB, Eisenach L, et al. Alkaline quinone flow battery. Science. 2015; 349(6255):1529-1532. https://doi.org/10.1126/science.aab3033 PMid:26404834.
14. Liang Y, Jing Y, Gheytani S, Lee K-Y, Liu P, Facchetti A, *et al.* Universal quinone electrodes for long-cycle-life aqueous rechargeable batteries. Nat Mater. 2017; 16(8):841-848. https://doi.org/10.1038/nmat4919 PMid:286281
15. Kwabi DG, Lin K, Ji Y, Kerr EF, Goulet M-A, De Porcellinis D, *et al.* Alkaline quinone flow battery with long lifetime at pH 12. Joule. 2018; 2(9):1894-1906. https://doi.org/10.1016/j.joule.2018.07.005 https://doi.org/10.1016/j.

joule.2018.08.013
16. Jin S, Jing Y, Kwabi DG, Ji Y, Tong L, De Porcellinis D, *et al*. A water-miscible quinone flow battery with high volumetric capacity and energy density. ACS Energy Letters. 2019; 4(6):1342-1348. https://doi.org/10.1021/acsenergylett.9b00739
17. Ji Y, Goulet M-A, Pollack DA, Kwabi DG, Jin S, De Porcellinis D, *et al*. A phosphonate-functionalized quinone redox flow battery at near-neutral pH with record capacity retention rate. Adv Energy Mater. 2019; 9(12):1900039. https://doi.org/10.1002/aenm.201900039
18. Wu M, Jing Y, Wong AA, Fell EM, Jin S, Tang Z, *et al*. Extremely stable anthraquinone negolytes synthesized from common precursors. Chem. 2020; 6(6):1432-1442. https://doi.org/10.1016/j.chempr.2020.03.021
19. Wang F, Sheng H, Li W, Gerken JB, Jin S, Stahl SS. Stable tetrasubstituted quinone redox reservoir for enhancing decoupled hydrogen and oxygen evolution. ACS Energy Lett. 2021; 6(4):1533-1539. https://doi.org/10.1021/acsenergylett.1c00236 PMid:34017916 PMCid:PMC8130882.
20. Kim JY, Ho J-W, Kim D, Moon M-W, Choi GH, Yoo PJ. Unveiling dominant impact of electrochemical stability on performance deterioration in alkaline redox flow batteries utilizing different benzoquinone derivatives. J Power Sources. 2024; 611:234766. https://doi.org/10.1016/j.jpowsour.2024.234766
21. Winsberg J, Hagemann T, Janoschka T, Hager MD, Schubert US. Redox-flow batteries: From metals to organic redox-active materials. Angew Chem Int Edition. 2017; 56(3):686-711. https://doi.org/10.1002/anie.201604925 PMid:28070964 PMCid:PMC5248651.
22. Nguyen TP, Easley AD, Kang N, Khan S, Lim SM, Rezenom YH, *et al*. Polypeptide organic radical batteries. Nature. 2021; 593(7857):61-66. https://doi.org/10.1038/s41586-021-03399-1 PMid:33953410.
23. Ye J, Xia L, Li H, de Arquer FPG, Wang H. The critical analysis of membranes toward sustainable and efficient vanadium redox flow batteries. Adv Mater. 2024; 36(28):2402090. https://doi.org/10.1002/adma.202402090 PMid:38776138.
24. Wang X, Lashgari A, Chai J, Jiang JJ. A membrane-free, aqueous/nonaqueous hybrid redox flow battery. Energy Storage Mater. 2022; 45:1100-1108. https://doi.org/10.1016/j.ensm.2021.11.008
25. Sharma J, Kulshrestha V. Advancements in polyelectrolyte membrane designs for vanadium redox flow battery (VRFB). Result Chem. 2023; 5:100892. https://doi.org/10.1016/j.rechem.2023.100892
26. Sharma J, Gupta R, Mishra S, Ramanujam K, Kulshrestha V. Sulfonated poly(2,6-dimethyl-1,4-phenylene ether)-modified mixed-matrix bifunctional polyelectrolyte membranes for long-run anthrarufin-based redox flow batteries. ACS Appl Mater Interfaces. 2023; 15(38):44899-44911. https://doi.org/10.1021/acsami.3c08089 PMid:37708403.
27. Chen R. Toward high-voltage, energy-dense, and durable aqueous organic redox flow batteries: Role of the supporting electrolytes. Chem Electro Chem. 2019; 6(3):603-612. https://doi.org/10.1002/celc.201801505
28. Wang L, Zhao Y, Fan B, Carta M, Malpass-Evans R, McKeown NB, *et al*. Polymer of intrinsic microporosity (PIM) films and membranes in electrochemical energy storage and conversion: A mini-review. Electrochem Commun. 2020; 118:106798. https://doi.org/10.1016/j.elecom.2020.106798
29. Sawant TV, Yim CS, Henry TJ, Miller DM, McKone JR. Harnessing interfacial electron transfer in redox flow batteries. Joule. 2021; 5(2):360-378. https://doi.org/10.1016/j.joule.2020.11.022
30. Park SJ, Hong MJ, Ha YJ, Choi J-I, Kim KJ. Two-in-one strategy for optimizing chemical and structural properties of carbon felt electrodes for vanadium redox flow batteries. Sci Technol Adv Mater. 2024; 25(1):2327274. https://doi.org/10.1080/14686996.2024.2327274 PMid:38529018 PMCid:PMC10962290.
31. Tseng TM, Huang RH, Huang CY, Liu CC, Hsueh KL, Shieu FS. Carbon felt coated with titanium dioxide/carbon black composite as negative electrode for vanadium redox flow battery. J Electrochem Soc. 2014; 161(6):A1132. https://doi.org/10.1149/2.102406jes
32. Nolte O, Volodin IA, Stolze C, Hager MD, Schubert US. Trust is good, control is better: A review on monitoring and characterization techniques for flow battery electrolytes. Mater Horiz. 2021; 8(7):1866-1925. https://doi.org/10.1039/D0MH01632B PMid:34846470.
33. Park M, Ryu J, Wang W, Cho J. Material design and engineering of next-generation flow-battery technologies. Nat Rev Mater. 2016; 2(1):16080. https://doi.org/10.1038/natrevmats.2016.80
34. Li Z, Lu Y-C. Advanced aqueous redox flow batteries design: Ready for long-duration energy storage applications? MRS Energy Sustain. 2022; 9(2):171-182. https://doi.org/10.1557/s43581-022-00027-x
35. Yang G, Zhu Y, Hao Z, Zhang Q, Lu Y, Yan Z, *et al*. An aqueous all-quinone-based redox flow battery employing neutral electrolyte. Adv Energy Mater. 2024; 14(26):2400022. https://doi.org/10.1002/aenm.202400022
36. Symons P. Quinones for redox flow batteries. Curr Opin Electrochem. 2021; 29:100759. https://doi.org/10.1016/j.coelec.2021.100759
37. Yang B, Hoober-Burkhardt L, Krishnamoorthy S, Murali A, Prakash GKS, Narayanan SR. High-performance aqueous organic flow battery with quinone-based redox couples at both electrodes. J Electrochem Soc. 2016; 163(7):A1442.

https://doi.org/10.1149/2.1371607jes
38. Wang C, Yang Z, Wang Y, Zhao P, Yan W, Zhu G, *et al*. High-performance alkaline organic redox flow batteries based on 2-hydroxy-3-carboxy-1,4-naphthoquinone. ACS Energy Lett. 2018; 3(10):2404-2409. https://doi.org/10.1021/acsenergylett.8b01296
39. Yang Z, Tong L, Tabor DP, Beh ES, Goulet M-A, De Porcellinis D, *et al*. Alkaline benzoquinone aqueous flow battery for large-scale storage of electrical energy. Adv Energy Mater. 2018; 8(8):1702056. https://doi.org/10.1002/aenm.201702056
40. Schlemmer W, Nothdurft P, Petzold A, Riess G, Frühwirt P, Schmallegger M, *et al*. 2-Methoxyhydroquinone from Vanillin for aqueous redox-flow batteries. Angew Chemie Int Ed. 2020; 59(51):22943-22946. https://doi.org/10.1002/anie.202008253 PMid:32815619 PMCid:PMC7891622.
41. Tong L, Goulet M-A, Tabor DP, Kerr EF, De Porcellinis D, Fell EM, *et al*. Molecular engineering of an alkaline naphthoquinone flow battery. ACS Energy Lett. 2019; 4(8):1880-1887. https://doi.org/10.1021/acsenergylett.9b01321
42. Schwan S, Schröder D, Wegner HA, Janek J, Mollenhauer D. Substituent pattern effects on the redox potentials of quinone-based active materials for aqueous redox flow batteries. Chem Sus Chem. 2020; 13(20):5480-5488. https://doi.org/10.1002/cssc.202000454 PMid:32798240 PMCid:PMC7702104.
43. Xia L, Zhang Y, Zhang H, Jiang S, Lv Q, Huo W, *et al*. Noncovalent interactions induced self-association in anthraquinone-iron aqueous redox flow batteries. Sustain Energy Fuels. 2022; 6(8):2045-2052. https://doi.org/10.1039/D1SE01895G
44. George TY, Kerr EF, Haya NO, Alfaraidi AM, Gordon RG, Aziz MJ. Size and charge effects on crossover of flow battery reactants evaluated by quinone permeabilities through Nafion. J Electrochem Soc. 2023; 170(4):040509. https://doi.org/10.1149/1945-7111/accb6b
45. Liu Y, Zhang P, Wu Z, Ding G, Song X, Ma J, *et al*. Biomimetic naphthoquinone zwitterion derivative with water-solubilising amino acid side chain for high-stability aqueous redox flow batteries. ACS Energy Lett. 2024; 9(2):586-593. https://doi.org/10.1021/acsenergylett.3c02530
46. Goulet M-A, Tong L, Pollack DA, Tabor DP, Odom SA, Aspuru-Guzik A, *et al*. Extending the lifetime of organic flow batteries via redox state management. J Am Chem Soc. 2019; 141(20):8014-8019. https://doi.org/10.1021/jacs.8b13295 PMid:30945536.
47. Murata T, Hamasaki M, Morita Y. A benzoquinone-imidazole hybrid organic anolyte for aqueous redox flow batteries. Chem Commun. 2024; 60(7):878-880. https://doi.org/10.1039/D3CC04840C PMid:38164888.
48. Clarindo JEdS, Colombo RNP, Sedenho GC, Faria LCI, Bertaglia T, Lima FCDA, *et al*. Molecular mechanism and electrostatic effect enabling symmetric all-quinone aqueous redox flow batteries. ACS Sustain Chem Eng. 2024; 12(31):11488-11497. https://doi.org/10.1021/acssuschemeng.3c08218
49. Lee W, Park G, Kwon Y. Alkaline aqueous organic redox flow batteries of high energy and power densities using mixed naphthoquinone derivatives. Chem Eng J. 2020; 386:123985. https://doi.org/10.1016/j.cej.2019.123985
50. Hofmann JD, Pfanschilling FL, Krawczyk N, Geigle P, Hong L, Schmalisch S, *et al*. Quest for organic active materials for redox flow batteries: 2,3-Diaza-anthraquinones and their electrochemical properties. Chem Mater. 2018; 30(3):762-774. https://doi.org/10.1021/acs.chemmater.7b04220
51. Chang D-R, Kim Y, Jung S. Comprehensive study of the performance of alkaline organic redox flow batteries as large-scale energy storage systems. Int J Energy Res. 2019; 43(9):4449-4458. https://doi.org/10.1002/er.4573
52. Lin K, Gómez-Bombarelli R, Beh ES, Tong L, Chen Q, Valle A, *et al*. A redox-flow battery with an alloxazine-based organic electrolyte. Nat Energy. 2016; 1(9):16102. https://doi.org/10.1038/nenergy.2016.102
53. Qian X, Chang D-R, Jung S. Experimental and computational study on alloxazine derivative-based organic redox flow battery. Chem Eng J. 2022; 429:132136. https://doi.org/10.1016/j.cej.2021.132136
54. Hollas A, Wei X, Murugesan V, Nie Z, Li B, Reed D, *et al*. A biomimetic high-capacity phenazine-based anolyte for aqueous organic redox flow batteries. Nat Energy. 2018; 3(6):508-514. https://doi.org/10.1038/s41560-018-0167-3
55. Park J, Lee Y, Yun D, Kim D, Hwang G, Han B, *et al*. A benzo[a]phenazine-based redox species with highly reversible two-electron reaction for aqueous organic redox flow batteries. Electrochimica Acta. 2023; 439:141644. https://doi.org/10.1016/j.electacta.2022.141644
56. Kong T, Li J, Wang W, Zhou X, Xie Y, Ma J, *et al*. Enabling long-life aqueous organic redox flow batteries with a highly stable, low redox potential phenazine anolyte. ACS Appl Mater Interfaces. 2024; 16(1):752-760. https://doi.org/10.1021/acsami.3c15238 PMid:38132704.
57. Liu Y, Zhang P, Wu Z, Wei J, Ding G, Song X, *et al*. Screening ultra-stable (phenazine)dioxyalkanocic acids with varied water-solubilising chain lengths for high-capacity aqueous redox flow batteries. J Am Chem Soc. 2024; 146(5):3293-3302. https://doi.org/10.1021/jacs.3c11887 PMid:38277694
58. Zhang C, Niu Z, Peng S, Ding Y, Zhang L, Guo X, *et al*. Phenothiazine-based organic catholyte for high-capacity and long-life aqueous redox flow batteries. Adv Mater. 2019; 31(24):1901052. https://doi.org/10.1002/adma.201901052
59. Martinez-Gonzalez E, Amador-Bedolla C, Ugalde-Saldivar VM. Reversible redox chemistry in a phenoxazine-based organic compound: A two-electron storage negolyte

for alkaline flow batteries. ACS Appl Energy Mater. 2022; 5(12):14748-14759. https://doi.org/10.1021/acsaem.2c02114

60. Fang X, Zeng L, Li Z, Robertson LA, Shkrob IA, Zhang L, *et al*. A cooperative degradation pathway for organic phenoxazine catholytes in aqueous redox flow batteries. Next Energy. 2023; 1(1):100008. https://doi.org/10.1016/j.nxener.2023.100008
61. Yin T, Duanmu J, Liu L. Viologen-based aqueous organic redox flow batteries: materials synthesis, properties, and cell performance. J Mater Chem A. 2024; 12(26):15519-15540. https://doi.org/10.1039/D4TA00753K
62. Huang J, Yang Z, Murugesan V, Walter E, Hollas A, Pan B, *et al*. Spatially constrained organic diquat anolyte for stable aqueous flow batteries. ACS Energy Lett. 2018; 3(10):2533-2538. https://doi.org/10.1021/acsenergylett.8b01550
63. DeBruler C, Hu B, Moss J, Luo J, Liu TL. A sulfonate-functionalized viologen enabling neutral cation exchange, aqueous organic redox flow batteries toward renewable energy storage. ACS Energy Lett. 2018; 3(3):663-668. https://doi.org/10.1021/acsenergylett.7b01302
64. Hu B, Tang Y, Luo J, Grove G, Guo Y, Liu TL. Improved radical stability of viologen anolytes in aqueous organic redox flow batteries. Chem Commun. 2018; 54(50):6871-6874. https://doi.org/10.1039/C8CC02336K PMid:29741542.
65. Liu Y, Li Y, Zuo P, Chen Q, Tang G, Sun P, *et al*. Screening viologen derivatives for neutral aqueous organic redox flow batteries. Chem Sus Chem. 2020; 13(9):2245-2249. https://doi.org/10.1002/cssc.202000381 PMid:32162480.
66. Ohira A, Funaki T, Ishida E, Kim J-D, Sato Y. Redox-flow battery operating in neutral and acidic environments with multielectron-transfer-type viologen molecular assembly. ACS Appl Energy Mater. 2020; 3(5):4377-4383. https://doi.org/10.1021/acsaem.0c00067
67. Liu L, Yao Y, Wang Z, Lu Y-C. Viologen radical stabilization by molecular spectators for aqueous organic redox flow batteries. Nano Energy. 2021; 84:105897. https://doi.org/10.1016/j.nanoen.2021.105897
68. Kathiresan M, Ambrose B, Angulakshmi N, Mathew DE, Sujatha D, Stephan AM. Viologens: A versatile organic molecule for energy storage applications. J Mater Chem A. 2021; 9(48):27215-27233. https://doi.org/10.1039/D1TA07201C
69. Korshunov A, Gibalova A, Gruenebaum M, Ravoo BJ, Winter M, Cekic-Laskovic I. Supramolecular viologen-cyclodextrin electrolytes for aqueous organic redox flow batteries. ACS Appl Energy Mater. 2021; 4(11):12353-12364. https://doi.org/10.1021/acsaem.1c02156
70. Korshunov A, Gibalova A, Grünebaum M, Ravoo BJ, Winter M, Cekic-Laskovic I. Host-guest interactions enhance the performance of viologen electrolytes for aqueous organic redox flow batteries. Batteries Supercaps. 2021; 4(6):923-928. https://doi.org/10.1002/batt.202100018
71. Martínez-González E, Flores-Leonar MM, Amador-Bedolla C, Ugalde-Saldívar VM. Concentration effects on the first reduction process of methyl viologens and diquat redox flow battery electrolytes. ACS Appl Energy Mater. 2021; 4(7):6624-6634. https://doi.org/10.1021/acsaem.1c00685
72. Li H, Fan H, Hu B, Hu L, Chang G, Song J. Spatial structure regulation: A rod-shaped viologen enables long lifetime in aqueous redox flow batteries. Angew Chemie Int Ed. 2021; 60(52):26971-26977. https://doi.org/10.1002/anie.202110010 PMid:34647654.
73. Pan M, Gao L, Liang J, Zhang P, Lu S, Lu Y, *et al*. Reversible redox chemistry in pyrrolidinium-based TEMPO radical and extended viologen for high-voltage and long-life aqueous redox flow batteries. Adv Energy Mater. 2022; 12(13):2103478. https://doi.org/10.1002/aenm.202103478
74. Nikumbe DY, Bavdane PP, Sreenath S, Paramasivam S, Pandi RG, Kumar SS, *et al*. Stability of monoradical cation dimer of viologen derivatives in aqueous redox flow battery. J Appl Electrochem. 2024; 54(10):2165-2177. https://doi.org/10.1007/s10800-024-02100-4
75. Lv X-L, Sullivan P, Fu H-C, Hu X, Liu H, Jin S, et al. Dextrosil-viologen: A robust and sustainable anolyte for aqueous organic redox flow batteries. ACS Energy Lett. 2022; 7(8):2428-2434. https://doi.org/10.1021/acsenergylett.2c01198
76. Ghahremani R, Dean W, Sinclair N, Shen X, Starvaggi N, Alfurayj I, *et al*. Redox-active eutectic electrolyte with viologen and ferrocene derivatives for flow batteries. ACS Appl Mater Interfaces. 2023; 15(1):1148-1156. https://doi.org/10.1021/acsami.2c18546 PMid:36563037.
77. Huang M, Hu S, Yuan X, Huang J, Li W, Xiang Z, *et al*. Five-membered-heterocycle bridged viologen with high voltage and superior stability for flow battery. Adv Funct Mater. 2022; 32(16):2111744. https://doi.org/10.1002/adfm.202111744
78. Borchers PS, Elbert J, Anufriev I, Strumpf M, Nischang I, Hager MD, *et al*. A viologen polymer and a compact ferrocene: Comparison of solution viscosities and their performance in a redox flow battery with a size exclusion membrane. Macromolecular Chem Phys. 2022; 223(2):2100373. https://doi.org/10.1002/macp.202100373
79. Gao M, Salla M, Song Y, Wang Q. High-power near-neutral aqueous all-organic redox flow battery enabled with a pair of anionic redox species. Angew Chemie Int Ed. 2022; 61(41):e202208223. https://doi.org/10.1002/anie.202208223 PMid:35997142.
80. Ambrose B, Naresh R, Kathiresan M, Ulaganathan M, Ragupathy P. Highly stable asymmetric viologen as an anolyte for aqueous organic and halide-based redox flow batteries. Energy Technol. 2023; 11(1):2201046. https://doi.org/10.1002/ente.202201046
81. Cho Y, Jang D, Park J-J, Kye H, Kwon JE, Kim B-G. Bipolar-type organic electrode material composed of a viologen-naphthalene diimide-viologen triad for

Li-organic batteries. ACS Appl Energy Mater. 2023. https://doi.org/10.1021/acsaem.3c02025
82. Ambrose B, Naresh R, Deshmukh S, Kathiresan M, Ragupathy P. Exploring contemporary advancements and outlook in viologen-based aqueous organic redox flow batteries: A mini review. Energy Fuels. 2023; 37(23):18226-18242. https://doi.org/10.1021/acs.energyfuels.3c02299
83. He X, Chen L, Baumgartner T. Modified viologen- and carbonylpyridinium-based electrodes for organic batteries. ACS Appl Mater Interfaces. 2023. https://doi.org/10.1021/acsami.3c09856 PMid:37584306.
84. Qu K, Liu Y, Hong D, Shen Z, Zhang X, Han X, *et al*. A highly soluble and readily accessible viologen negolyte for pH-neutral aqueous organic redox flow batteries. J Power Sources. 2024; 599:234222. https://doi.org/10.1016/j.jpowsour.2024.234222
85. Kim S, Kim D, Hwang G, Jeon J. A bromide-ligand ferrocene derivative redox species with high reversibility and electrochemical stability for aqueous redox flow batteries. J Electroanal Chem. 2020; 869:114131. https://doi.org/10.1016/j.jelechem.2020.114131
86. Zhao Z, Zhang B, Schrage BR, Ziegler CJ, Boika A. Investigations into aqueous redox flow batteries based on ferrocene bisulfonate. ACS Appl Energy Mater. 2020; 3(10):10270-10277. https://doi.org/10.1021/acsaem.0c02259
87. Yu J, Salla M, Zhang H, Ji Y, Zhang F, Zhou M, *et al*. A robust anionic sulfonated ferrocene derivative for pH-neutral aqueous flow battery. Energy Storage Materials. 2020; 29:216-222. https://doi.org/10.1016/j.ensm.2020.04.020
88. Chen Q, Li Y, Liu Y, Sun P, Yang Z, Xu T. Designer ferrocene catholyte for aqueous organic flow batteries. Chem Sus Chem. 2021; 14(5):1295-1301. https://doi.org/10.1002/cssc.202002467 PMid:33200881.
89. Luo J, Hu M, Wu W, Yuan B, Liu TL. Mechanistic insights of cycling stability of ferrocene catholytes in aqueous redox flow batteries. Energy Environ Sci. 2022; 15(3):1315-1324. https://doi.org/10.1039/D1EE03251H
90. Zhang B, Schrage BR, Frkonja-Kuczin A, Gaire S, Popov IA, Ziegler CJ, *et al*. Zwitterionic ferrocenes: An approach for redox flow battery (RFB) catholytes. Inorg Chem. 2022; 61(21):8117-8120. https://doi.org/10.1021/acs.inorgchem.2c00722 PMid:35584531.
91. Caianiello C, Arenas LF, Turek T, Wilhelm R. Characterization of an aqueous flow battery utilizing a hydroxylated tetracationic viologen and a simple cationic ferrocene derivative. Adv Energy Sustain Res. 2023; 4(10):2300077. https://doi.org/10.1002/aesr.202300077
92. Giri S, Dash I. Ferrocene to functionalized ferrocene: a versatile redox-active electrolyte for high-performance aqueous and non-aqueous organic redox flow batteries. J Mater Chem A. 2023; 11(31):16458-16493. https://doi.org/10.1039/D3TA01747H
93. Liu Y, Goulet M-A, Tong L, Liu Y, Ji Y, Wu L, *et al*. A long-lifetime all-organic aqueous flow battery utilising TMAP-TEMPO radical. Chem. 2019; 5(7):1861-1870. https://doi.org/10.1016/j.chempr.2019.04.021
94. Liu B, Tang CW, Jiang H, Jia G, Zhao T. Carboxyl-functionalized TEMPO catholyte enabling high-cycling-stability and high-energy-density aqueous organic redox flow batteries. ACS Sustain Chem Eng. 2021; 9(18):6258-6265. https://doi.org/10.1021/acssuschemeng.0c08946
95. Nambafu GS, Siddharth K, Zhang C, Zhao T, Chen Q, Amine K, *et al*. An organic bifunctional redox-active material for symmetric aqueous redox flow battery. Nano Energy. 2021; 89:106422. https://doi.org/10.1016/j.nanoen.2021.106422
96. Fan H, Wu W, Ravivarma M, Li H, Hu B, Lei J, *et al*. Mitigating ring-opening to develop stable TEMPO catholytes for ph-neutral all-organic redox flow batteries. Adv Funct Mater. 2022; 32(33):2203032. https://doi.org/10.1002/adfm.202203032
97. Pedraza E, de la Cruz C, Mavrandonakis A, Ventosa E, Rubio-Presa R, Sanz R, *et al*. Unprecedented aqueous solubility of TEMPO and its application as high capacity catholyte for aqueous organic redox flow batteries. Adv Energy Mater. 2023; 13(39):2301929. https://doi.org/10.1002/aenm.202301929
98. Seo N-U, Kim K, Yeo J, Kwak SJ, Kim Y, Kim H, *et al*. Covalent conjugation of a 'hydroxide-philic' functional group achieving 'hydroxide-phobic' TEMPO with superior stability in all-organic aqueous redox flow batteries. J Mater Chem A. 2023; 11(35):18953-18963. https://doi.org/10.1039/D3TA03420H
99. Chen R. Redox flow batteries: Mitigating cross-contamination via bipolar redox-active materials and bipolar membranes. Curr Opin Electrochem. 2023; 37:101188. https://doi.org/10.1016/j.coelec.2022.101188
100. Chen C, Zhang S, Zhu Y, Qian Y, Niu Z, Ye J, et al. Pyridyl group design in viologens for anolyte materials in organic redox flow batteries. RSC Adv. 2018; 8(34):18762-18770. https://doi.org/10.1039/C8RA02641F PMid:35539647 PMCid:PMC9080602.
101. Chai J, Lashgari A, Cao Z, Williams CK, Wang X, Dong J, *et al*. PEGylation-enabled extended cyclability of a non-aqueous redox flow battery. ACS Appl Mater Interfaces. 2020; 12(13):15262-15270. https://doi.org/10.1021/acsami.0c01045 PMid:32150369.
102. Back J, Kwon G, Byeon JE, Song H, Kang K, Lee E. Tunable redox-active triazenyl-carbene platforms: A new class of anolytes for non-aqueous organic redox flow batteries. ACS Appl Mater Interfaces. 2020; 12(33):37338-37345. https://doi.org/10.1021/acsami.0c09400 PMid:32692157.
103. Li M, Case J, Minteer SD. Bipolar redox-active molecules in non-aqueous organic redox flow batteries: Status and challenges. Chem Electro Chem. 2021; 8(7):1215-1232. https://doi.org/10.1002/celc.202001584

104. Zhu Y, Yang F, Niu Z, Wu H, He Y, Zhu H, *et al*. Enhanced cyclability of organic redox flow batteries enabled by an artificial bipolar molecule in neutral aqueous electrolyte. J Power Sources. 2019; 417:83-89. https://doi.org/10.1016/j.jpowsour.2019.02.021
105. Borchers PS, Strumpf M, Friebe C, Nischang I, Hager MD, Elbert J, *et al*. Aqueous redox flow battery suitable for high temperature applications based on a tailor-made ferrocene copolymer. Adv Energy Mater. 2020; 10(41):2001825. https://doi.org/10.1002/aenm.202070168
106. Hagemann T, Strumpf M, Schröter E, Stolze C, Grube M, Nischang I, *et al*. (2,2,6,6-Tetramethylpiperidin-1-yl)oxyl-containing zwitterionic polymer as catholyte species for high-capacity aqueous polymer redox flow batteries. Chem Mater. 2019; 31(19):7987-7999. https://doi.org/10.1021/acs.chemmater.9b02201
107. Wu W, Luo J, Wang F, Yuan B, Liu TL. A self-trapping, bipolar viologen bromide electrolyte for redox flow batteries. ACS Energy Lett. 2021; 6(8):2891-2897. https://doi.org/10.1021/acsenergylett.1c01146
108. Liu Y, Dai G, Chen Y, Wang R, Li H, Shi X, *et al*. Effective design strategy of small bipolar molecules through fused conjugation toward 2.5 V based redox flow batteries. ACS Energy Lett. 2022; 7(4):1274-1283. https://doi.org/10.1021/acsenergylett.2c00198 PMid:35572819 PMCid:PMC9097584.
109. Wang L, Huang M, Wan K, Fu Z, Xiang Z, Liang Z. Highly soluble TEMPO-viologen bipolar molecule for ultra-stable aqueous redox flow batteries. Adv Funct Mater. 2024; 34(11):2310620. https://doi.org/10.1002/adfm.202310620
110. De Porcellinis D, Mecheri B, D'Epifanio A, Licoccia S, Granados-Focil S, Aziz MJ. Communication-sulfonated poly (ether ketone) as cation exchange membrane for alkaline redox flow batteries. J Electrochem Soc. 2018; 165(5):A1137. https://doi.org/10.1149/2.1291805jes
111. Zhang L, Zhang S, Li E, Zhao L, Zhang S. Sulfonated poly(ether ketone) membrane for quinone-based organic flow batteries. J Membrane Sci. 2019; 584:246-253. https://doi.org/10.1016/j.memsci.2019.05.008
112. Li Y, Liu Y, Xu Z, Yang Z. Poly(phenylene oxide)-based ion-exchange membranes for aqueous organic redox flow battery. Ind Eng Chem Res. 2019; 58(25):10707-10712. https://doi.org/10.1021/acs.iecr.9b01377
113. Wang A, Tan R, Liu D, Lu J, Wei X, Alvarez-Fernandez A, *et al*. Ion-selective microporous polymer membranes with hydrogen-bond and salt-bridge networks for aqueous organic redox flow batteries. Adv Mater. 2023; 35(12):2210098. https://doi.org/10.1002/adma.202210098 PMid:36634684.
114. Zhang B, Yang Z, Liu Q, Liu Y, Jiang S, Zhang X, *et al*. High-performance aqueous organic redox flow battery enabled by sulfonated anthrone-containing poly(aryl ether ketone) membranes. J Membrane Sci. 2024; 706:122968. https://doi.org/10.1016/j.memsci.2024.122968
115. Robb BH, George TY, Davis CM, Tang Z, Fujimoto CH, Aziz MJ, *et al*. Sulfonated diels-alder poly(phenylene) membrane for efficient ion-selective transport in aqueous metalorganic and organic redox flow batteries. J Electrochem Soc. 2023; 170(3):030515. https://doi.org/10.1149/1945-7111/acbee6
116. Hou J, Liu Y, Liu Y, Wu L, Yang Z, Xu T. Self-healing anion exchange membrane for pH7 redox flow batteries. Chem Eng Sci. 2019; 201:167-174. https://doi.org/10.1016/j.ces.2019.02.033
117. Tsehaye MT, Yang X, Janoschka T, Hager MD, Schubert US, Alloin F, *et al*. Study of anion exchange membrane properties incorporating n-spirocyclic quaternary ammonium cations and aqueous organic redox flow battery performance. Membranes [Internet]. 2021; 11(5). https://doi.org/10.3390/membranes11050367 PMid:34070143 PMCid:PMC8158339.
118. Sharma J, Kulshrestha V. Degradation mechanisms of anion exchange membranes due to alkali hydrolysis and radical oxidative species. Alkaline Anion Exchange Membranes for Fuel Cells. 2024. pp. 241-284. https://doi.org/10.1002/9783527837588.ch11
119. Sharma J, Khan H, Upadhyay P, Kothandaraman R, Kulshrestha V. Stable poly(2,6-dimethyl-1,4-phenylene ether) based cross-linked cationic polyelectrolyte membrane with ionic microstructure modification for efficient VRFB performance. ACS Appl Energy Mater. 2023; 6(1):447-460. https://doi.org/10.1021/acsaem.2c03421
120. Sreenath S, Nayanthara PS, Pawar CM, Noufal MC, Nagarale RK. Phenolic triamine dangling poly(VDF-co-HFP) anion exchange membrane for all aqueous organic redox flow battery. J Energy Storage. 2021; 40:102689. https://doi.org/10.1016/j.est.2021.102689
121. Shukla G, Kumbhar G, Bruggeman C, Curley SJ, Szczepanski CR, Hickey DP, *et al*. Poly(vinylidene difluoride-co-hexafluoropropylene) grafted with polyether amphoteric ion-exchange membranes for aqueous redox flow batteries. ACS Appl Energy Mater. 2024. https://doi.org/10.1021/acsaem.4c00014
122. Sharma J, Totee C, Kulshrestha V, Ameduri B. Spectroscopic evidence and mechanistic insights on dehydrofluorination of PVDF in alkaline medium. Eur Polym J. 2023; 201:112580. https://doi.org/10.1016/j.eurpolymj.2023.112580
123. Mishra S, Sharma J, Upadhyay P, Kulshrestha V. 2-Acrylamido-2-methylpropane sulfonic acid (AMPS) grafted poly(vinylidene fluoride) (PVDF) membrane for improved vanadium redox flow battery (VRFB) performance. Next Energy. 2024; 5:100164. https://doi.org/10.1016/j.nxener.2024.100164
124. Liu J, Wu W, Zuo P, Yang Z, Xu T. Ultramicroporous Tröger's base framework membranes for pH-neutral aqueous organic redox flow batteries. ACS Macro

Lett. 2024; 13(3):328-334. https://doi.org/10.1021/acsmacrolett.4c00011 PMid:38436221.
125. Song W, Peng K, Xu W, Liu X, Zhang H, Liang X, *et al*. Upscaled production of an ultramicroporous anion-exchange membrane enables long-term operation in electrochemical energy devices. Nature Communications. 2023; 14(1):2732. https://doi.org/10.1038/s41467-023-38350-7 PMid:37169752 PMCid:PMC10175247.
126. Rathod NH, Sharma J, Raj SK, Yadav V, Rajput A, Kulshrestha V. Fabrication of a stable and efficient bipolar membrane by incorporation of nano-mos2 interfacial layer for conversion of salt into corresponding acid and alkali by water dissociation using electrodialysis. ACS Sustain Chem Eng. 2020; 8(34):13019-13029. https://doi.org/10.1021/acssuschemeng.0c04010
127. Yan Z, Wycisk RJ, Metlay AS, Xiao L, Yoon Y, Pintauro PN, *et al*. High-voltage aqueous redox flow batteries enabled by catalyzed water dissociation and acid-base neutralization in bipolar membranes. ACS Cent Sci. 2021; 7(6):1028-1035. https://doi.org/10.1021/acscentsci.1c00217 PMid:34235263 PMCid:PMC8228583.
128. Wei X, Cosimbescu L, Xu W, Hu JZ, Vijayakumar M, Feng J, *et al*. Towards high-performance nonaqueous redox flow electrolyte via ionic modification of active species. Adv Energy Mater. 2015; 5(1):1400678. https://doi.org/10.1002/aenm.201400678
129. Wang W, Xu W, Cosimbescu L, Choi D, Li L, Yang Z. Anthraquinone with tailored structure for a nonaqueous metal-organic redox flow battery. Chemical Commun. 2012; 48(53):6669-6671. https://doi.org/10.1039/c2cc32466k PMid:22641051
130. Huang J, Yang Z, Vijayakumar M, Duan W, Hollas A, Pan B, *et al*. A two-electron storage nonaqueous organic redox flow battery. Adv Sustain Syst. 2018; 2(3):1700131. https://doi.org/10.1002/adsu.201700131
131. Wei X, Xu W, Huang J, Zhang L, Walter E, Lawrence C, *et al*. Radical compatibility with nonaqueous electrolytes and its impact on an all-organic redox flow battery. Angew Chemie Int Ed. 2015; 54(30):8684-8687. https://doi.org/10.1002/anie.201501443 PMid:25891480
132. Kim D-H, Seo S-J, Lee M-J, Park J-S, Moon S-H, Kang YS, *et al*. Pore-filled anion-exchange membranes for non-aqueous redox flow batteries with dual-metal-complex redox shuttles. J Membrane Sci. 2014; 454:44-50. https://doi.org/10.1016/j.memsci.2013.11.051
133. Li Y, Sniekers J, Malaquias JC, Van Goethem C, Binnemans K, Fransaer J, *et al*. Crosslinked anion exchange membranes prepared from poly(phenylene oxide) (PPO) for non-aqueous redox flow batteries. J Power Sources. 2018; 378:338-344. https://doi.org/10.1016/j.jpowsour.2017.12.049
134. Peltier CR, Rhodes Z, Macbeth AJ, Milam A, Carroll E, Coates GW, *et al*. Suppressing crossover in nonaqueous redox flow batteries with polyethylene-based anion-exchange membranes. ACS Energy Lett. 2022; 7(11):4118-4128. https://doi.org/10.1021/acsenergylett.2c01551
135. Small LJ, Pratt HD, Fujimoto CH, Anderson TM. Diels alder polyphenylene anion exchange membrane for nonaqueous redox flow batteries. J Electrochem Soc. 2016; 163(1):A5106. https://doi.org/10.1149/2.0141601jes
136. Lehmann ML, Tyler L, Self EC, Yang G, Nanda J, Saito T. Membrane design for non-aqueous redox flow batteries: Current status and path forward. Chem. 2022; 8(6):1611-1636. https://doi.org/10.1016/j.chempr.2022.04.005
137. Manzoor Bhat Z, Furquan M, Aurang Zeb Gul Sial M, Alam U, Saeed Alzahrani A, Qamar M. Implications of electrode modifications in aqueous organic redox flow batteries. J Energy Chem. 2024; 95:499-510. https://doi.org/10.1016/j.jechem.2024.03.058
138. Lee W, Kwon BW, Kwon Y. Effect of carboxylic acid-doped carbon nanotube catalyst on the performance of aqueous organic redox flow battery using the modified alloxazine and ferrocyanide redox couple. ACS Appl Mater Interfaces. 2018; 10(43):36882-36891. https://doi.org/10.1021/acsami.8b10952 PMid:30299074.
139. Gao F, Cai X, Huang C. The impact of modified electrode on the performance of an DHAQ/ K4Fe(CN)6 redox flow battery. Electrochimica Acta. 2021; 390:138847. https://doi.org/10.1016/j.electacta.2021.138847
140. Mirle C, Medabalmi V, Ramanujam K. Crossover-free hydroxy-substituted quinone anolyte and potassium ferrocyanide catholyte for aqueous alkaline organic redox flow battery. Catalysis Today. 2021; 370:173-180. https://doi.org/10.1016/j.cattod.2020.12.012
141. Mirle C, Ramanujam K. On capacity upgradation and *in situ* capacity rebalancing in Anthrarufin-based alkaline redox flow batteries. ACS Appl Energy Mater. 2022; 5(8):9711-9721. https://doi.org/10.1021/acsaem.2c01392
142. Sharma J, Khan H, Upadhyay P, Rajak AK, Mishra S, Gayathri M N, *et al*. Robust sulfonated proton exchange membrane from a poly(styrene-co-divinylbenzene) melt-interpenetrated polyethylene network for vanadium redox flow batteries. ACS Appl Energy Mater. 2024. https://doi.org/10.1021/acsaem.4c01583
143. Tsehaye MT, Mourouga G, Schmidt TJ, Schumacher JO, Velizarov S, Van der Bruggen B, *et al*. Towards optimised membranes for aqueous organic redox flow batteries: Correlation between membrane properties and cell performance. Renew Sustain Energy Rev. 2023; 173:113059. https://doi.org/10.1016/j.rser.2022.113059